# Diffusive Transport Modelling of Corrosion Agents through the Engineered Barrier System in a Deep Geological Repository for Used Nuclear Fuel

NWMO-TR-2018-06 May 2018

**Scott Briggs**

**Magdalena Krol**

York University, Canada

nwmo
NUCLEAR WASTE MANAGEMENT ORGANIZATION
SOCIÉTÉ DE GESTION DES DÉCHETS NUCLÉAIRES

**Nuclear Waste Management Organization**
22 St. Clair Avenue East, 6th Floor
Toronto, Ontario
M4T 2S3
Canada

Tel: 416-934-9814
Web: www.nwmo.ca

# Diffusive Transport Modelling of Corrosion Agents through the Engineered Barrier System in a Deep Geological Repository for Used Nuclear Fuel

## NWMO-TR-2018-06

May 2018

**Scott Briggs**
**Magdalena Krol**

Civil Engineering Department
Lassonde School of Engineering
York University, Canada

This report has been prepared under contract to NWMO. The report has been reviewed by NWMO, but the views and conclusions are those of the authors and do not necessarily represent those of the NWMO.

All copyright and intellectual property rights belong to NWMO.

**Document History**

| | | | |
|---|---|---|---|
| Title: | Diffusive Transport Modelling of Corrosion Agents through the Engineered Barrier System in a Deep Geological Repository for Used Nuclear Fuel | | |
| Report Number: | NWMO-TR-2018-06 | | |
| Revision: | R000 | Date: | May 2018 |
| York University, Canada | | | |
| Authored by: | Scott Briggs | | |
| Reviewed and Approved by: | Magdalena Krol | | |
| Nuclear Waste Management Organization | | | |
| Reviewed by: | Jeff Binns<br>Mehran Behazin<br>Jennifer McKelvie<br>Peter Keech | | |
| Accepted by: | Paul Gierszewski | | |

## ABSTRACT

**Title:** **Diffusive Transport Modelling of Corrosion Agents through the Engineered Barrier System in a Deep Geological Repository for Used Nuclear Fuel**
**Report No.:** **NWMO-TR-2018-06**
**Author(s):** Scott Briggs, Magdalena Krol
**Company:** York University, Canada
**Date:** May 2018

The Nuclear Waste Management Organization (NWMO) is developing a deep geological repository (DGR) as part of Adaptive Phased Management (APM), Canada's plan for long-term management of used nuclear fuel. The DGR will rely on a multiple barrier system to protect people and the environment. To contain and isolate radionuclides, an engineered barrier system (EBS) will be constructed within a low permeability host rock. The EBS will comprise used fuel containers (UFCs) surrounded by bentonite clay. The purpose of this project is to develop a numerical model to estimate sulphide transport through bentonite assuming a constant source of microbiologically influenced corrosion (MIC) products and examine its effect on the copper coated UFC.

This report outlines the development of a three-dimensional (3D) numerical transport model, using COMSOL Multiphysics (version 5.3), with easily changeable parameters for scoping calculations. The model is capable of simulating the diffusion of corrosive compounds through the bentonite buffer under thermal and variably-saturated conditions. The transport modelling of corrosive compounds provides information that can assist in the establishment of a MIC allowance for the UFC design and the developed model can be applied to a variety of scoping scenarios.

The simulations presented here consider the geometry of the current NWMO EBS design, as well as, predicted repository environmental conditions for a generic repository site. Results show that corrosion from sulphide diffusion is not uniform over the container, as would be predicted using one-dimensional (1D) calculations. In all cases, 3D modelling predicts zones of higher corrosion at the hemi-spherical end caps due to geometry effects. This results from the unique geometry of the placement room and UFC, resulting in complex sulphide diffusion pathways moving radially inwards to the hemi-spherical UFC end caps. This work highlights the need for using 3D geometry to model sulphide transport in the Canadian repository.

Due to the changing nature of the DGR, the model was developed for various DGR conditions: 1) isothermal and fully saturated 2) non-isothermal and fully saturated, and 3) isothermal and variably saturated. For each condition, a constant, 1 ppm sulphide concentration boundary condition was assumed at the far-field source. However, this condition, as well as other parameters will be refined as design-specific information becomes available and will incorporate site-specific data derived from the NWMO site selection process. For the isothermal (25°C), fully saturated condition, the estimated corrosion rate was 0.76 nm/year/ppm of sulphide. Corrosion rates are reported for unit sulphide concentrations, however the results scale linearly for different sulphide concentrations as expected from Fick's Law of Diffusion (implemented in the model). The model also predicted that the time required for sulphide to saturate the bentonite was approximately 2,000 years. Consideration of thermal effects, where long-term temperatures approach 11°C, resulted in a corrosion rate of 0.53 nm/year/ppm sulphide. Finally, the variably saturated module predicted full water saturation of the DGR at approximately 2,000 years with the first saturated pathways to the UFC surface appearing around 200 years.

TABLE OF CONTENTS

Page

ABSTRACT ..... iii

1. INTRODUCTION ..... 1

2. MECHANISMS OF COPPER CORROSION IN THE DEEP SUBSURFACE ..... 3

2.1 CORROSION ..... 3

3. METHODOLOGY ..... 4

3.1 DIFFUSION MODULE ..... 5
3.2 TEMPERATURE MODULE ..... 5
3.3 RICHARDS EQUATION MODULE ..... 7

4. SUBSURFACE MODELLING ..... 8

4.1 DIFFUSION MODULE PARAMETERS ..... 9
4.2 THERMAL MODULE PARAMETERS ..... 13
4.3 RICHARDS EQUATION MODULE PARAMETERS ..... 15

5. RESULTS ..... 16

5.1 DIFFUSION MODULE RESULTS ..... 16
5.1.1 Validation Results ..... 16
5.1.2 Modelling Results ..... 18
5.1.3 Sensitivity Analysis ..... 20
5.2 THERMAL MODULE RESULTS ..... 22
5.3 RICHARDS EQUATION MODULE RESULTS ..... 26

6. DISCUSSION AND FUTURE WORK ..... 28

ACKNOWLEDGMENTS ..... 29

REFERENCES ..... 30

## LIST OF TABLES

**Page**

Table 1: Thermal Parameters for DGR Materials .....6
Table 2: Thermal Output of Used Fuel .....6
Table 3: Properties of modelled bentonite (Baumgartner, 2006) .....8
Table 4: Model Validation: Analytical vs. COMSOL.....17
Table 5: Corrosion rates for and UFC package and placement room.....20
Table 6: Corrosion rates for thermal module .....25

## LIST OF FIGURES

**Page**

Figure 1: Canadian deep geological repository design concept for the long-term management of used nuclear fuel. .....1
Figure 2: Conceptual design of a copper coated used fuel container inside the lower bentonite block.....3
Figure 3: COMSOL generated geometry of a single UFC within a bentonite buffer. .....9
Figure 4: Conceptual Design of a Copper Engineering Barrier System (reproduced from NWMO, 2013) including bentonite of various engineered forms (ex. Highly compacted bentonite, bentonite pellets (gap fill) and dense back fill). .....10
Figure 5: COMSOL generated geometry of a 10 m segment of a single placement room, containing 13 UFCs and surrounding bentonite. .....10
Figure 6: a) COMSOL generated geometry of a 10 m segment of a single placement room taking advantage of symmetry to minimize computation requirements. Figure b) shows the symmetry boundary condition in blue. Figure c) shows the no flow boundary condition in green which also acts as a symmetrical boundary condition. .....11
Figure 7: Sulphide flux sensitivity due to two different mesh implementations looking at both average and maximum rates. The results shown are from a UFC package simulation. ....13
Figure 8: The thermal model tracks diffusion within the DGR under heated conditions. The DGR consists of three types of bentonite: HCB immediately surrounding the UFC, bentonite spacer blocks between UFCs and bentonite pellets material used to fill the remaining gaps in the placement room. .....14
Figure 9: The thermal model includes the surrouding host rock allowing heat to dissipate from the DGR. .....14
Figure 10: The DGR mesh included 2.8 million elements (left) and the DGR (in blue) plus host rock mesh included 4.1 million elements (right). .....15
Figure 11: A 2D model geometry on the right approximates the 3D DGR on the left. Saturation, representing initial conditions, is shown on the right image. .....15
Figure 12: Richards equation module mesh including 8443 elements with higher resolution in the placement room and a coarser mesh moving away from the DGR. .....16
Figure 13: Illustrative of 2D cylindrical shell diffusion with unit height, highlighting the larger outer perimeter of the bentonite cover. The figure illustrates the complexities of radial diffusion towards cylindrical surfaces.....18
Figure 14: Corrosion rate for the case of a single UFC package. Maximum corrosion occurs at the hemi-spherical end cap. .....19
Figure 15: Corrosion rate for the case of a 10 m segment of a placement room containing 13 UFCs. .....19
Figure 16: Maximum corrosion rate for varying effective sulphide diffusion coefficients in the placement room geometry. .....21

Figure 17: Maximum corrosion rate for varying sulphide concentration gradients in the placement room geometry. ....21
Figure 18: Sulphide flux at the UFC surface for isothermal conditions at 11°C. ....22
Figure 19: Time dependent sulphide flux for the isothermal model at 11°C over 1,000,000 years. Minimum flux occurs at the inner UFC surface (between two containers) while the maximum flux occurs at the hemi-spherical end caps. ....23
Figure 20: Temperature dependent model showing the average UFC surface temperature over 1,000,000 years. ....24
Figure 21: Time and temperature dependent corrosion rates in the DGR for the thermal module. For the maximum reported values (red line), corrosion rates peak around 1,000 years at 2.48 nm/year/ppm sulphide then drop to a steady state value of 0.53. ....25
Figure 22: a) Corrosion rate for 1 ppm sulphide concentration gradient for a hydraulic conductivity of $10^{-14}$ m/s b) Sulphide flux profile through placement room at peak corrosion rate. ....26
Figure 23: Saturation at 10, 100 and 1,000 years for varying hydraulic conductivities. ....27

## 1. INTRODUCTION

The Nuclear Waste Management Organization (NWMO) is implementing Adaptive Phased Management (APM), the approach selected by the Government of Canada in 2007 for long-term management of used nuclear fuel. The goal of APM is long-term containment and isolation of used nuclear fuel in a Deep Geological Repository (DGR) constructed in a suitable formation in either sedimentary or crystalline rock at a depth of approximately 500 meters. In support of APM, the NWMO is pursuing an active Technical Program addressing a wide range of relevant topics in collaboration with Canadian universities, consultants and other countries pursuing the development of DGRs for used nuclear fuel. NWMO's Technical Program is currently refining generic engineering designs and safety cases in support of APM.

The design of a DGR includes an engineered barrier system (EBS) within a suitably low permeability rock that acts as a natural barrier. Within a placement room, the EBS comprises a used fuel container (UFC) surrounded by highly compacted bentonite (HCB) clay (Figure 1). Canada's current UFC design has 3 mm of copper applied directly by electrodeposition and cold spray onto a steel container that holds 48 used CANadian Deuterium Uranium (CANDU) nuclear bundles.

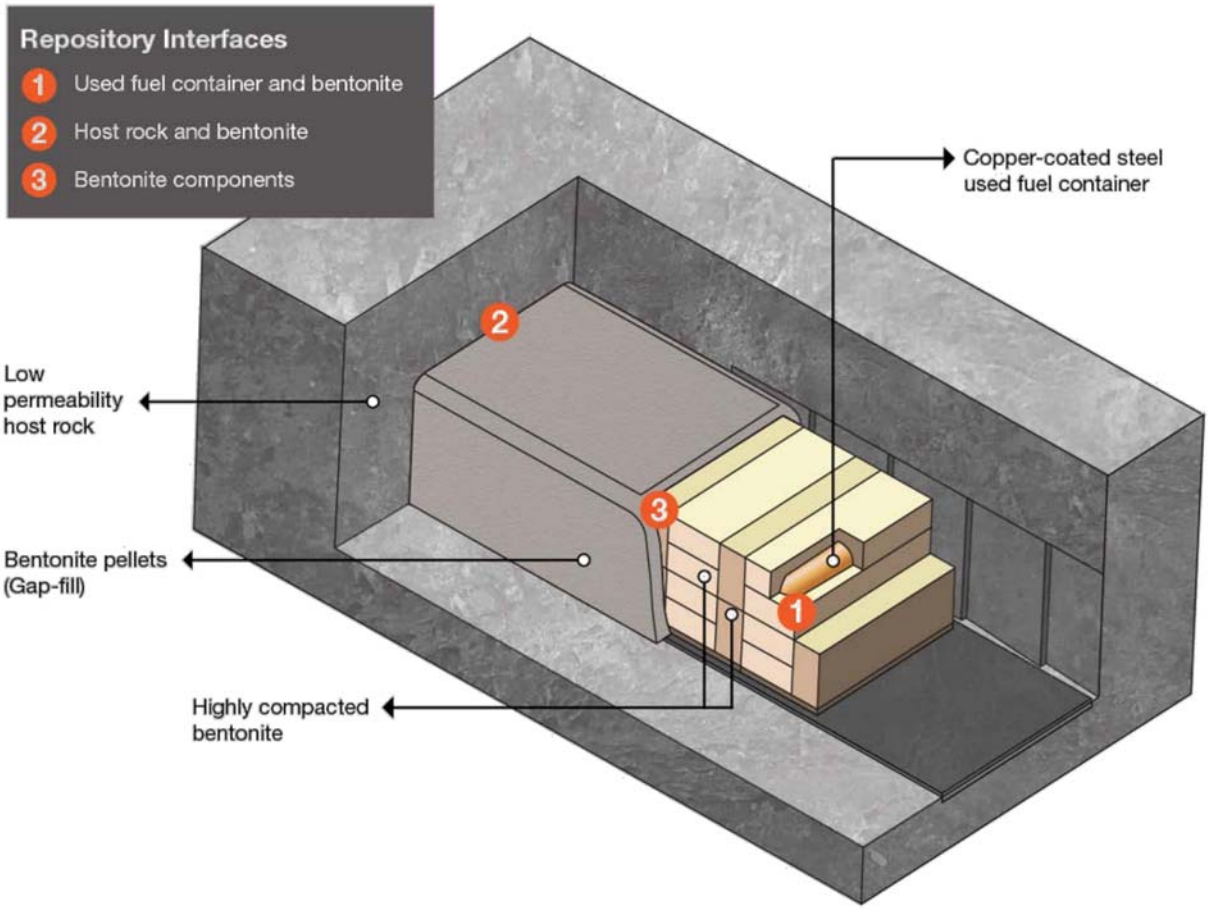



**Figure 1: Canadian deep geological repository design concept for the long-term management of used nuclear fuel.**

The purpose of this report is to showcase a numerical model that has been developed to estimate sulphide transport through bentonite assuming a constant source of microbiologically influenced corrosion (MIC) products under different repository conditions, and examine its effect on the copper coated UFC. The developed model will be refined as design-specific information becomes available and will incorporate site-specific data through the NWMO site selection process. From previous investigations, it is anticipated that two possible forms of copper MIC in a repository could occur: stress corrosion cracking (SCC) and general corrosion. Microbial activity produces SCC agents (e.g., ammonia, acetate and nitrite) and sulphide, which could potentially promote both SCC and general corrosion. Previous microbial modelling indicated that the concentration of SCC agents (nitrite, acetate, and ammonia) reaching the container surface would be low and unlikely to cause SCC (King and Kolar, 2006; Ikeda and Litke, 2007, 2008; Litke and Ikeda, 2008, 2011). The expected absence of SCC is supported by conceptual stress models, as the tensile stresses required for SCC are absent in a DGR (Kwong, 2011). Therefore, in this report, SCC is not considered and copper corrosion is assumed to be primarily caused by general, uniform corrosion due to sulphide resulting in MIC. In addition, no microbial, corrosion, or geochemical reactions are considered. The model presented in this report simulates sulphide diffusion under different conditions from the host rock, through the bentonite to the UFC.

Previous studies have estimated the rate of uniform anaerobic corrosion of copper containers to be 1 nm per year based on the assumption that sulphate-reducing bacteria (SRB) in the repository far-field would provide a continuous source concentration of at most 3 ppm of sulphide (King, 1996). Accordingly, the total depth of uniform corrosion based on this value, using a 1D approach, is predicted to be 1 mm after 1 million years (King, 1996; Scully and Edwards, 2013) using a bentonite thickness of 40 cm and a diffusion coefficient of $1x10^{-11}$ $m^2/s$ for sulphide in bentonite. However, using the same conservative value for sulphide, MIC estimates made on a site-specific and design-specific basis could experience higher levels of corrosion. For example, the NWMO UFC design has a cylindrical shaped container with hemi-spherical end caps. This design, when placed within a bentonite buffer package, would require a 3D modelling approach due to the complex geometry. In addition, repository conditions such as temperature and saturation could affect corrosion rates.

The activities described in this report focus on the development of a 3D model, using COMSOL Multiphysics (version 5.3) which is capable of estimating the diffusive transport of sulphide in the DGR, refining previous MIC scoping calculations and assisting in the establishment of a MIC allowance for the UFC design. The development of the model assumed certain conditions. First, near field sources of MIC products within the bentonite are assumed to be negligible since the engineered bentonite is designed to suppress microbial activity (Stroes-Gascoyne et al., 2010; Bengtsson and Pederson, 2017). Second, advective groundwater flow through the bentonite is assumed to be negligible as the host rock is assumed to act as a low permeability barrier and therefore the transport of MIC substances is assumed to be diffusion dominated (Alt-Epping et al., 2015; Bourg et al., 2008). Third, it is assumed that diffusion is governed by Fick's First Law and controlled by an effective diffusion coefficient that represents the transport of sulphide through bentonite accounting for various processes including tortuosity and porosity. Lastly, no microbial or geochemical reactions were incorporated into the model, and therefore the model represents a conservative estimate of MIC at the container.

This report outlines the details of the 3D numerical model, including the description of the simulated domain, assumptions, and results. It is broken up into three sections: isothermal

modelling (Section 4.1), thermal simulations (Section 4.2), and variably saturated simulations (Section 4.3). It concludes with a summary and recommendations.

## 2. MECHANISMS OF COPPER CORROSION IN THE DEEP SUBSURFACE

### 2.1 CORROSION

The NMWO UFC design consists of a copper-coated steel container that is cylindrical with hemi-spherical ends. The design includes a copper layer of approximately 3 mm, which is more than twice the current 1,000,000 year reference corrosion allowance of 1.3 mm (NWMO, 2013). The UFC is emplaced within two blocks of highly compacted bentonite (Figure 2, top block not shown) then horizontally placed within a crystalline or sedimentary rock excavation and finally backfilled with granular bentonite (Figure 1).

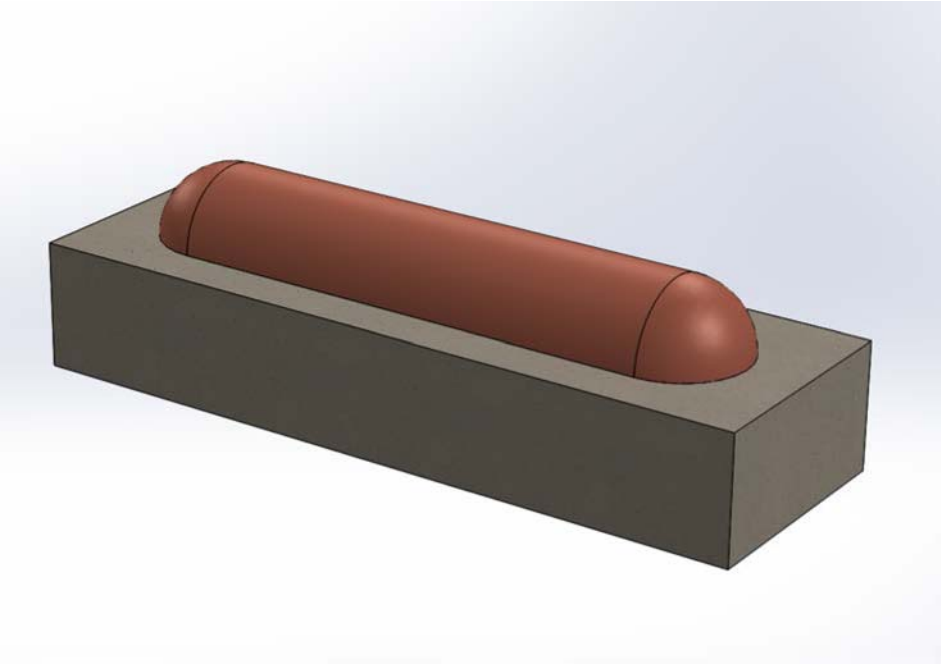


**Figure 2: Conceptual design of a copper coated used fuel container inside the lower bentonite block.**

Following closure and sealing of the DGR the bentonite buffers will eventually saturate with groundwater from the surrounding host rock leading to the onset of copper corrosion driven initially by $O_2$ reduction. It is expected that 11.9 mol of $O_2$ per container will be trapped in the DGR as a result of excavation and placement activities leading to a uniform copper corrosion depth of 75.5 µm (Hall, 2017). Notably, this corrosion depth is highly conservative as it ignores other $O_2$ sinks within the DGR (e.g. mineral oxidation and aerobic microbial activity). Following this brief oxic stage, the DGR will re-establish anoxic conditions under which uniform copper corrosion can proceed in the presence of $H_2O$, $Cl^-$ or $HS^-$. When reacting with water (Equation 1) hydrogen gas may be produced, however this reaction is thermodynamically unfavourable (Kwong, 2011, Johansson, 2012, Ottosson, 2017), and can be suppressed by a hydrogen partial pressure of just $10^{-6}$ mbar.

$$Cu_{(s)} + H_2O \rightleftarrows Cu^{+}_{(aq)} + \frac{1}{2}H_{2(g)} + OH^{-} \qquad \text{Equation 1}$$

In the presence of $Cl^-$, copper can be dissolved to form cuprous (Cu(I)) complexes $CuCl_2^-$ or $CuCl_3^{2-}$ (Equation 2). However, this reaction is also thermodynamically unfavourable, and can be suppressed by small amounts of hydrogen (Bojinov and Mäkelä, 2003).

$$\boldsymbol{Cu_{(s)}\, nCl^- + H_2O \rightleftarrows [CuCl_n]_{(aq)}^{(n-1)-} + OH^- + \frac{1}{2}H_{2(g)}} \qquad \text{Equation 2}$$

This reaction (Equation 2) is of a slightly higher concern in sedimentary host rocks, where higher $Cl^-$ levels are expected (i.e. around 5-6 molar, Kwong 2011). However, owing to the extremely low water content, the limited mobility of corrosion products in bentonite, and the presence of small amounts of hydrogen, the impact of such a reaction is greatly mitigated, such that negligible corrosion is expected from this mechanism.

In the presence of $HS^-$ copper can corrode via Equation 3:

$$\boldsymbol{2Cu_{(s)} + HS^- + H^+ \rightleftarrows Cu_2S_{(s)} + H_{2(g)}} \qquad \text{Equation 3}$$

In this case, the reaction is thermodynamically favourable; thus, copper corrosion via sulphide is the most likely of the three reactions. However, this corrosion mechanism is limited by the transport of sulphide species to the container surface. It is assumed that any sulphide present at the host rock-bentonite buffer interface (and not inside the bentonite) is due to the activity of sulphate reducing bacteria (SRB) in the host rock. This is because the engineered bentonite is designed to suppress microbial activity (Stroes-Gascoyne et al., 2010; Bengtsson and Pederson, 2017). Therefore, sulphide species must diffuse through the bentonite in order to reach the container surface to cause corrosion.

The depth of copper corrosion (at any given time) [$LT^{-1}$] can be calculated based on molar conversion and stoichiometric conversion ratio of hydrogen sulphide to copper sulphide (SKB, 2010):

$$d_{corr} = \frac{N_{HS} f_{HS} M_{cu}}{A_{corr} \rho_{cu}} \qquad \text{Equation 4}$$

where $N_{HS}$ is the amount of sulphide [$NT^{-1}$] determined from the model, $f_{HS}$ is the stoichiometric factor (with a value of 2 from the stoichiometry of Equation 3), $M_{cu}$ is the molar mass of copper [$MN^{-1}$], $A_{corr}$ is the area exposed to corrosion [$L^2$] and $\rho_{cu}$ is the density of copper [$ML^{-3}$].

## 3. METHODOLOGY

As described in the introduction, the current diffusive transport model is capable of simulating different repository conditions. The model has evolved from a simple 1D model to a 3D isothermal, saturated model. Complexities were implemented sequentially, as described below. The current numerical model consists of three modules depending on the desired conditions to be simulated. All modules simulate the diffusion of sulphide under these various conditions:

1. Diffusion in an isothermal, saturated environment (referred to as the Diffusion Module);
2. Non-isothermal and fully saturated environment (referred to as the Thermal Module); and
3. Isothermal and variably saturated environment (referred to as the Richard's Equation Module).

These modules consist of different geometries, boundary conditions, initial conditions, and physical parameters dependent on the implementation. The Diffusion Module assumes isothermal conditions and diffusion dominated transport. The Thermal Module includes temperature dependent diffusion coefficients. Finally, the Richards Equation Module includes movement of water in variably saturated media. Each module is developed and reported separately.

### 3.1 DIFFUSION MODULE

The transport of corrosion products is assumed to be diffusion dominated due to the low permeability the bentonite buffer used in the EBS. The bentonite chosen for the EBS is Wyoming MX-80 which has a high smectitic content and therefore a high swelling capacity. This bentonite is expected to develop a very low hydraulic conductivity such that diffusion will be the dominant transport mechanism (Alt-Epping et al., 2015; Bourg et al., 2008). Diffusion is described by Fick's First Law:

$$J = -D\nabla C \qquad \text{Equation 5}$$

where $J$ is the diffusive flux [$NL^{-2}T^{-1}$], $D$ is the effective diffusion coefficient [$L^2T^{-1}$], and $\nabla C$ is the concentration of the substance [$NL^{-3}$] over a distance [L] and calculated using:

$$D = \tau\varepsilon_a D_o \qquad \text{Equation 6}$$

The sulphide diffusion coefficient in water ($D_o$, free diffusion) was taken to be $10^{-9}$ $m^2/s$ at 25°C (Lide and Haynes, 2009; Chen et al, 2011). The effective transport porosity ($\varepsilon_a$), a subset of the total porosity, representing the fraction of pores in which sulphide is transported, was assumed to be 0.1 (King et al, 2008). Tortuosity ($\tau$) of the bentonite buffer was assumed to be 0.1, therefore the effective diffusion coefficient was $10^{-11}$ $m^2/s$ (Oscarson et al., 1994). Development of the anion diffusion mechanisms, for example the double layer theory controlling the effective diffusion porosity and tortuosity, is outside the scope of this report (Bradbury and Baeyens, 2003; Van Loon et al., 2007; Appelo et al., 2010; Glaus et al., 2011; Appelo, 2013; Alt-Epping et al., 2015). Furthermore, speciation of sulphide will occur under different pH conditions. For example, $H_2S$ diffusion would be more probable under neutral conditions while $HS^-$ would be likely under more basic conditions (Morse et al., 1987). However, the current model assumes no geochemical reactions occur within the bentonite. Since diffusion is temperature dependent, temperature effects were considered in the second module (Martin et al., 2000; Idemitsu et al., 2016).

### 3.2 TEMPERATURE MODULE

The first module of the model assumed isothermal conditions. However, the repository is expected to warm in the short term due to the presence of the used nuclear fuel. In the long term, the DGR will cool to background host rock levels. In this study, the average ground level temperature was assumed to be 5°C, with a geothermal gradient of 0.012°C per meter of depth (Baumgartner et al., 1994). Therefore, at 500 m below ground surface, the background temperature was assumed to be 11°C. It was also assumed that the sulphide diffusion coefficient decreased with decreasing temperature, controlled by the viscosity of water as described by the Stokes-Einstein equation (Einstein, 1905):

$$\frac{D_{T_1}}{D_{T_2}} = \frac{T_1}{T_2}\frac{\mu_{T_2}}{\mu_{T_1}} \qquad \text{Equation 7}$$

where $D$ is the diffusion coefficient, $T_1$ and $T_2$ are the respective temperatures and $\mu$ is the dynamic viscosity of water. The viscosity of water increases with decreasing temperatures and was calculated following the method described in Huber et al. (2009). The assumed 11°C at 500 m below ground surface results in a drop in the sulphide diffusion coefficient from $1 \times 10^{-11}$ $m^2/s$ (25°C) to $6.7 \times 10^{-12}$ $m^2/s$.

The transient heat equation was used to model time dependent conduction of heat:

$$\rho c_p \frac{\partial T}{\partial t} = \nabla(k \cdot \nabla T) + q(t) \qquad \text{Equation 7}$$

where $T$ is temperature [Θ], $k$ is the material thermal conductivity [$MLT^{-3}\Theta^{-1}$], $c_p$ is the material specific heat capacity [$L^2MT^{-2}\Theta^{-1}$], $\rho$ is the material density [$ML^{-3}$] and $q$ is a time dependent heat source [$ML^2T^{-3}$]. Thermal properties for bentonite are determined by calculations described by Baumgartner (2006) and shown in Table 1. The thermal output, $q$, of the used nuclear fuel container was determined based on 30-year-old fuel at time of placement (Tait et al., 2000) and shown in Table 2.

**Table 1:** Thermal Parameters for DGR Materials

| Property | Thermal Conductivity (W/m°C) | Specific Heat (J/kg°C) | Bulk Density ($kg/m^3$) |
|---|---|---|---|
| Crystalline DGR | 3.0 | 845 | 2700 |
| Highly Compacted Bentonite | 1.0 | 1280 | 1955 |
| Bentonite Spacer Blocks | 2.0 | 1060 | 2276 |
| Bentonite Pellet Material | 0.4 | 870 | 1439 |
| Steel UFC | 60.5 | 434 | 7750 |

**Table 2:** Thermal Output of Used Fuel Bundles per Container

| Time (years) | Heat Source (W) |
|---|---|
| Discharge | $1.3 \times 10^6$ |
| 10 | 260 |
| 20 | 203 |
| 30 | 169 |
| 40 | 142 |
| 50 | 122 |
| 60 | 105 |
| 75 | 85.9 |
| 100 | 65.3 |
| 150 | 46.1 |
| 200 | 38.7 |
| 300 | 32.8 |
| 500 | 26.8 |
| 1,000 | 18.6 |
| 10,000 | 6.59 |
| 100,000 | 0.38 |
| 1,000,000 | 0.14 |
| 10,000,000 | 0.09 |

### 3.3 RICHARDS EQUATION MODULE

The next complexity that was introduced into the model was variably saturated conditions. This module includes transient water saturation using Richards equation under isothermal conditions. Richards equation describes the movement of water, while assuming the air phase is at atmospheric pressure and any changes in air pressure do not affect the flow of water. Therefore, using this approach does not result in a fully coupled two-phase flow model but allows for a first approximation of variably saturated conditions. COMSOL simulates variably saturated flow using Richards equation expressed in terms of pressure head as follows (Bear, 2012):

$$(C_m + SeS)\frac{\partial H_p}{\partial t} + \nabla \cdot \left(-K\nabla\left(H_p + D\right)\right) = 0 \qquad \text{Equation 8}$$

where $C_m$ is the specific moisture capacity (see Equation 11), *Se* is the effective saturation of the bentonite (see Equation 11), *S* is the storage coefficient [$LM^{-1}T^2$], $H_p$ is the pressure head [L], *t* is time [T], *K* is the hydraulic conductivity (see Equation 11) and *D* is the depth of the system [L]. The dependent variable, pressure (*p*) [$L^{-1}MT^{-2}$], is related to the pressure head by:

$$H_p = \frac{p}{\rho g} \qquad \text{Equation 9}$$

where $\rho$ is the density [$ML^{-3}$] of water (assumed to be 1000 kg/$m^3$) and *g* is the acceleration due to gravity [$LT^{-2}$].

Richards equation models the flow of water in the bentonite, where any pore may or may not be completely saturated. The amount of water within a pore is represented by the volumetric water content, $\theta$ (ratio of water volume to total volume). The terms, $C_m$, *Se* and *K* from Equation 8 vary with pressure head and with $\theta$ resulting in a non-linear model. K is the relative hydraulic conductivity and is given by:

$$K = K_S k_r \qquad \text{Equation 10}$$

where $K_s$ is the saturated hydraulic conductivity [$LT^{-1}$] and $k_r$ is the relative permeability (see Equation 11). To describe $\theta$, $C_m$, *Se* and $k_r$, the van Genuchten (1980) relationships were used.

$$\theta = \begin{cases} S_{Ir} + Se(\varepsilon - S_{Ir}) & H_p < 0 \\ \varepsilon & H_p \geq 0 \end{cases}$$

$$Se = \begin{cases} \dfrac{1}{\left(1 + \left|\alpha H_p\right|^n\right)^m} & H_p < 0 \\ 1 & H_p \geq 0 \end{cases}$$

$$C_m = \begin{cases} \dfrac{\propto m}{1-m}(\varepsilon - S_{Ir}) Se^{\frac{1}{m}}\left(1 - Se^{\frac{1}{m}}\right)^m & H_p < 0 \\ 0 & H_p \geq 0 \end{cases}$$

$$k_r = \begin{cases} Se^{0.5}\left(1 - \left(1 - Se^{\frac{1}{m}}\right)^m\right)^2 & H_p < 0 \\ 1 & H_p \geq 0 \end{cases}$$

Equation 11

where $\alpha$, *n* and *m* are constants associated with the material properties (Table 3) and where *m* = *1-1/n*. The modelled system is unsaturated for values of $H_p$ less than zero and saturated when the fluid pressure is atmospheric (*Hp* ≥ *0*).

Although Richard's equation models bentonite saturation, sulphide transport within the bentonite is still assumed to be diffusion dominated resulting in the combined equation:

$$\theta \frac{\partial c}{\partial t} + cC_m \frac{\partial H_p}{\partial t} + \nabla \cdot \left(-D_{eff} \nabla c\right) = 0 \qquad \text{Equation 12}$$

where $c$ is the concentration of sulphide, and the effective diffusion coefficient is defined:

$$D_{eff} = \frac{\theta}{\tau} D° \qquad \text{Equation 13}$$

where $D°$ is the free water diffusion coefficient. The diffusion coefficient of sulphide in water was assumed to be $1 \times 10^{-9}$ $m^2/s$ at 25°C (Lide and Haynes, 2009; Chen et al., 2011). The effective diffusion coefficient in bentonite is a function of saturation, porosity and tortuosity where the tortuosity model was chosen after Millington and Quirk (1961):

$$\tau = \theta^{-7/3} \varepsilon^2 \qquad \text{Equation 14}$$

where $\tau$ is the tortuosity, $\theta$ is the saturation and $\varepsilon$ is the porosity.

Material properties are taken from literature, specific to the highly compacted bentonite (HCB) that NWMO will use in a future DGR (Guo, 2017). It was assumed that the bentonite pellets placed between the host-rock and HCB has the same properties as the HCB. Therefore, a bentonite dry density of 1700 kg/m$^3$ was assumed for the entire system. The van Genuchten and hydraulic parameters are shown in Table 3.

**Table 3: Properties of modelled bentonite (Baumgartner, 2006)**

| Property | Bentonite |
|---|---|
| Dry density | 1700 kg/m$^3$ |
| van Genuchten properties | |
| $\alpha$ | 0.0198 |
| $n$ | 1.545 |
| $m$ | 1-1/n |
| Irreducible water content ($S_{ir}$) | 0.001 |
| Total porosity ($\varepsilon$) | 0.382 |
| Tortuosity ($\tau$) | $\theta^{-7/3}\varepsilon^2$ |
| Initial saturation | 65 % |
| Hydraulic conductivity ($K_s$) | $6 \times 10^{-14}\ m/s$ |

Since Richards Equation does not track the movement of gas, any gas formation and movement would not be captured in this model.

## 4. SUBSURFACE MODELLING

The following section describes the modelled geometries, meshes, and computational techniques. Section 4.1 has been published in Briggs et al., (2017b); Briggs et al., (2017d), Section 4.2 in Briggs et al., (2017c) and Section 4.3 in Briggs et al., (2017a).

## 4.1 DIFFUSION MODULE PARAMETERS

The geometries for all modelling scenarios presented in this report follow the current NWMO reference design. The UFC package geometry consists of a bentonite buffer surrounding a cylindrical UFC with hemi-spherical ends (Figure 3). The UFCs, approximately 2.5 m long with a 0.56 m diameter are placed within the HCB buffer box to produce a 1 x 1 x 2.8 $m^3$ package. These packages will then be moved to a placement room with a height of approximately 3.2 m and a width of approximately 2.2 m (NWMO, 2013). The geometry of the UFC and surrounding bentonite results in a minimum bentonite coverage of the UFC of 0.3 m.

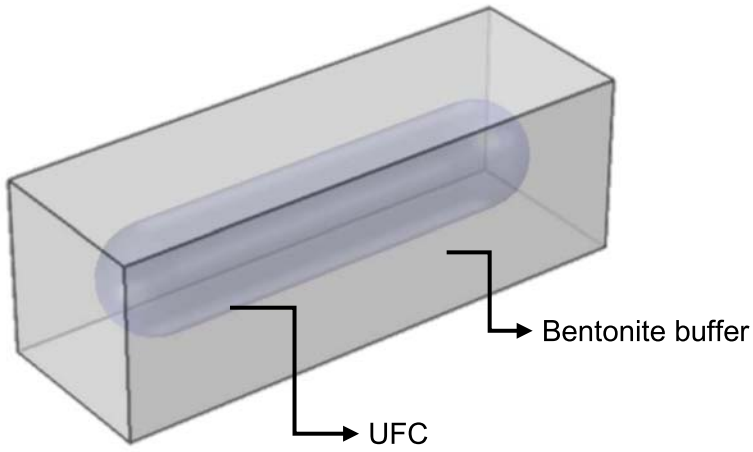



**Figure 3: COMSOL generated geometry of a single UFC within a bentonite buffer.**

The placement room is approximately 300 m long (depending on the host rock), however, due to symmetry it is sufficient to model only a fraction of this length. Therefore, the placement room is represented by a 10 m segment (Figure 4). The placement room geometry also incorporates some aspects of the drilling process such as the 'lookouts' that are produced by the drilling method (Figure 4 and Figure 5). The lookouts refer to the slight angle at which the placement rooms are drilled and excavated at 5 m intervals. Within the placement room, each UFC package is separated by bentonite blocks with spacing specific to the thermal design requirements of the EBS. The placement room geometry and the respective UFC package spacing used in the present model is associated with the crystalline rock design parameters (Guo, 2017).

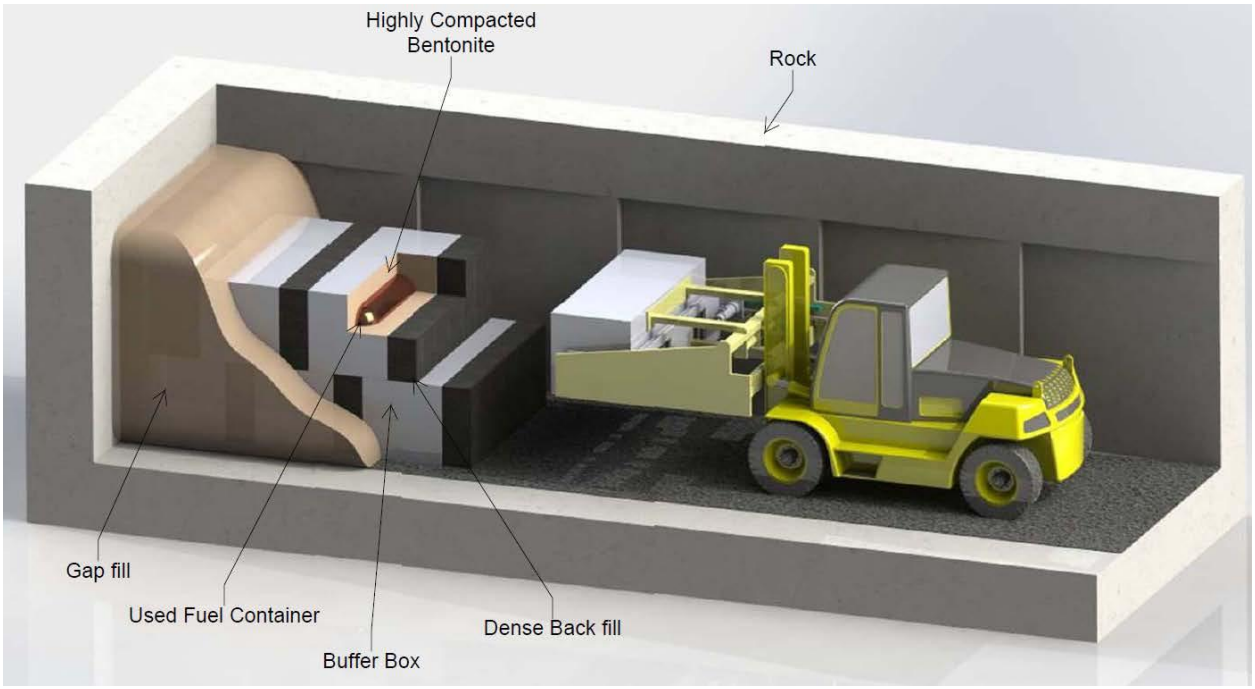



**Figure 4: Conceptual Design of a Copper Engineering Barrier System (reproduced from NWMO, 2013) including bentonite of various engineered forms (ex. Highly compacted bentonite, bentonite pellets (gap fill) and dense back fill).**

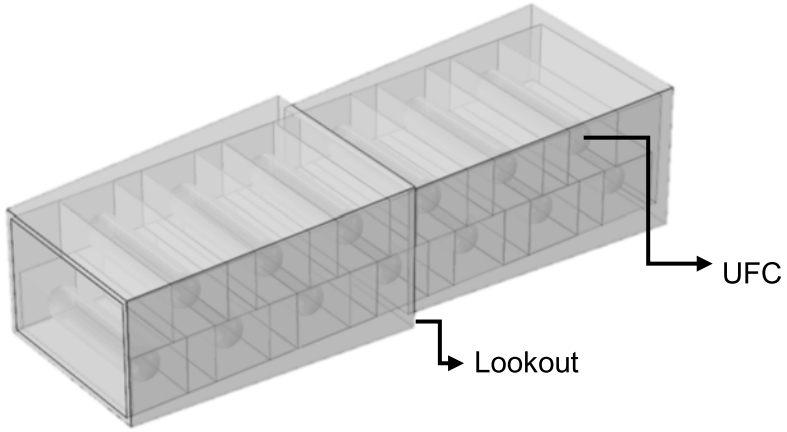



**Figure 5: COMSOL generated geometry of a 10 m segment of a single placement room, containing 13 UFCs and surrounding bentonite.**

For all modules, the far field sulphide concentration has been assumed to be 1 ppm and is applied as a constant concentration boundary condition around the perimeter of the placement room at the DGR-host rock interface. Since the actual value of sulphide in DGR groundwater is not yet known, the value was chosen as unity (1 ppm) to allow simple conversion when a DGR site has been chosen and pore water sampled. The expected concentrations of sulphide in a Canadian repository are over an order of magnitude lower (i.e. 30-90 ppb) (Gascoyne, 1997; Kremer, 2017). The rate of sulphide transport through the bentonite, as governed by Fick's Law, is linearly proportional to the sulphide concentration.

The UFC surface is also modelled as a constant sulphide concentration boundary condition with a prescribed value of 0 ppm. The 0 ppm concentration arises from the assumption that MIC is transport limited, and instantly consumes the sulphide via the copper corrosion reaction; resulting in no accumulation of sulphide at the UFC surface. The use of concentration boundary conditions results in a flux being reported at both boundaries. The flux, or amount of sulphide over time, is used to calculate a depth of corrosion over time using Equation 4. In reality, the copper sulphide layer formed via the corrosion reaction is very insoluble, and likely to present a physical barrier to sulphide ingress as it grows.

A COMSOL generated geometry is shown in Figure 6a) and includes 13 UFCs. Due to symmetries in the design of a single placement room, it is unnecessary to model the entire room. Therefore, a plane of symmetry is placed along the length of the placement room to reduce the computation load (Figure 6b)). In addition, at the left and right ends of the modelling domain (Figure 6c)), a no flux condition is prescribed to represent the symmetrical boundary condition between adjacent segments along the placement room.

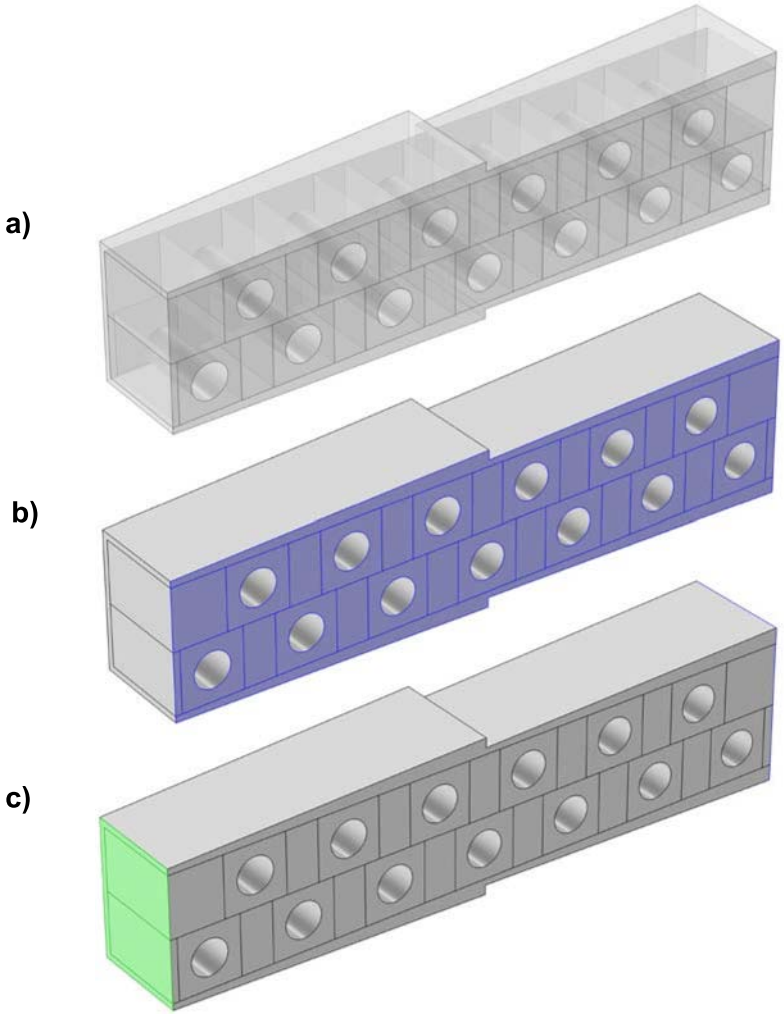



**Figure 6: a) COMSOL generated geometry of a 10 m segment of a single placement room taking advantage of symmetry to minimize computation requirements. Figure b) shows the symmetry boundary condition in blue. Figure c) shows the no flow boundary condition in green which also acts as a symmetrical boundary condition.**

In order to solve the system of partial differential equations in COMSOL, a finite element mesh was generated. The size and shape of the mesh is chosen as to minimize the number of finite elements needed while maximizing solution accuracy. The dimensionality and topology of the model geometry affect the optimal mesh selection. Accuracy within 1% of the analytical solution requires relatively modest computational requirements while accuracy within 0.1% can require significant computational time, even for simple geometries.

Finite elements require that the mesh strictly matches the desired model geometry in order to maximize accuracy. The size of the mesh element also plays a role in accuracy and it is generally best practice to reduce the size of a finite element in areas of complex geometry or near areas where high gradients are expected when solving the partial differential equations. In this report the corrosion rate at the UFC surface is desired therefore, the accuracy of the solution near the surface is a high priority. However, due to the semi-spherical cap on the UFC package there are multiple methods to mesh the geometry. Therefore, a combination of mesh element geometries were tested and compared on the UFC package. The first mesh consists of a thin boundary layer of curved hexahedra (bricks) shaped mesh elements adjacent to the UFC surface. The remainder of the cross section was populated with tetrahedral elements. This method is referred to as the Boundary Mesh in Figure 7. The second meshing method uses tetrahedral elements throughout the geometry and an automatic scaling method is applied adjacent to the UFC to approximately double the number of elements in this area. This mesh geometry is referred to as the Scaled Mesh (Figure 7). The Boundary Mesh and Scaled Mesh were generated using the same element properties, including minimum size, maximum size and growth rate.

Given the physics and geometry of the UFC package, both meshes resulted in slightly different solutions at a given maximum element size (Figure 7). As the mesh elements were refined, the respective solutions converged from opposite directions, one from larger and one from smaller flux values. This result showed that the upper and lower bound fluxes for the UFC converge to within 1% at the smallest mesh sizes tested. Similar mesh geometries for the placement room model indicated a convergence within 5%, the additional discrepancy is due to a relatively coarser mesh. The placement room geometry is larger and requires significantly more elements to model the geometry than the single UFC.

In general, the models in this report use finite element meshes that result in convergence within the 1% error for smaller models and 5% for larger models.

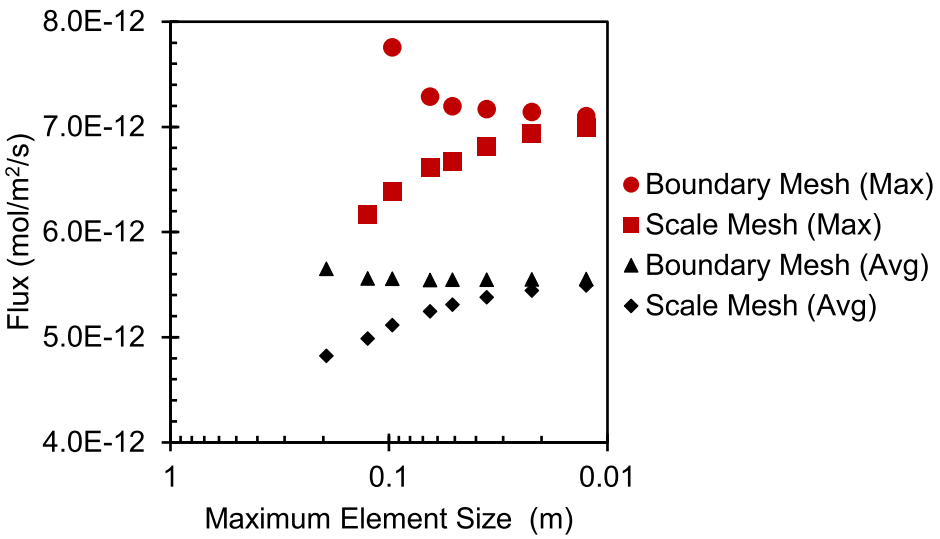



**Figure 7: Sulphide flux sensitivity due to two different mesh implementations looking at both average and maximum rates. The results shown are from a UFC package simulation.**

### 4.2 THERMAL MODULE PARAMETERS

The thermal module developed replicates the NMWO DGR design as published by Guo (2017), which consists of a placement room 3.2 m wide by 2.2 m tall and a few hundred meters deep depending on the host rock at the time of site selection. The UFC and HCB were separated by bentonite spacer blocks (0.5 m thickness) and backfilled with bentonite pellets. Each placement room was separated by 20 m of host rock. Due to the symmetrical layout of hundreds of UFCs it was sufficient to model a small fraction of the placement room to minimize computations (Figure 8).

For the time dependent thermal module, 10 m of host rock was included to represent a symmetrical segment of the 20 m placement rom spacing. The model also extended 500 m to the surface and 10,000 m below ground level to minimize boundary effects (Figure 9). Similar to the diffusion module, the sulphide concentration is set to zero at the UFC surface and 1 ppm at the DGR-host rock interface.

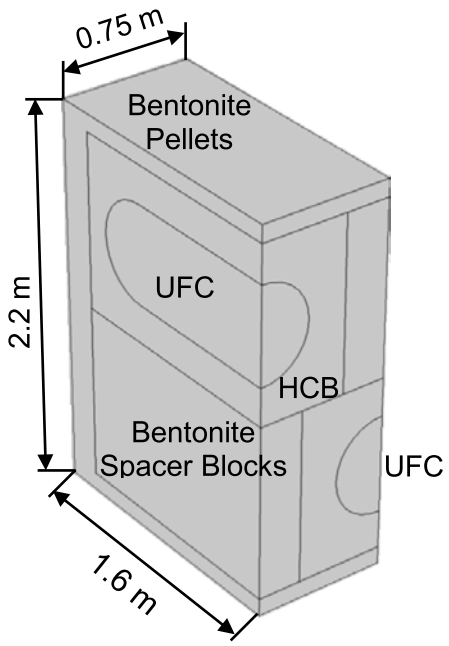



**Figure 8: The thermal model tracks diffusion within the DGR under heated conditions. The DGR consists of three types of bentonite: HCB immediately surrounding the UFC, bentonite spacer blocks between UFCs and bentonite pellets material used to fill the remaining gaps in the placement room.**

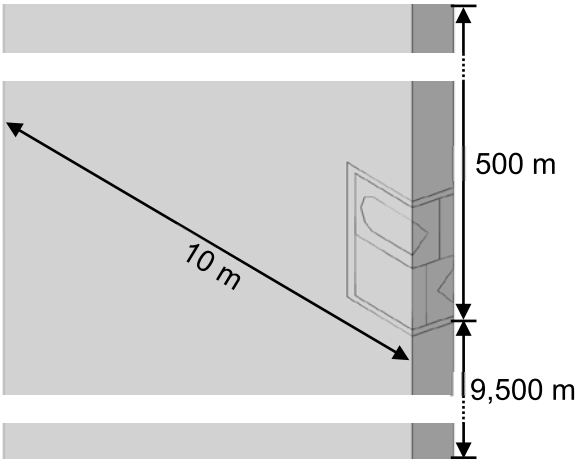



**Figure 9: The thermal model includes the surrouding host rock allowing heat to dissipate from the DGR.**

The model consists of a finer mesh within the DGR to effectively capture the sulphide diffusion, while the mesh in the host rock becomes progressively larger away from the placement room to reduce computation requirements (Figure 10). The DGR mesh consist of 2.8 million elements while the larger geometry model, including the host rock, consist of 4.1 million elements.

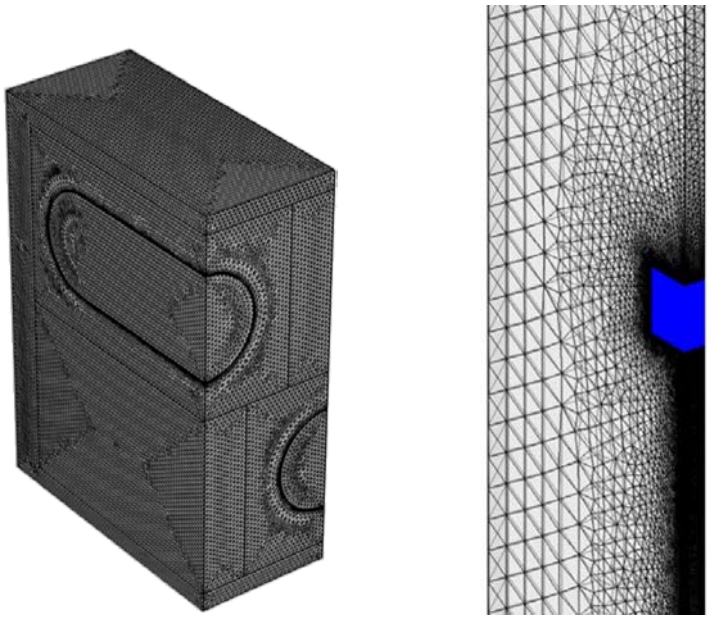


**Figure 10: The DGR mesh included 2.8 million elements (left) and the DGR (in blue) plus host rock mesh included 4.1 million elements (right).**

### 4.3 RICHARDS EQUATION MODULE PARAMETERS

The Richards equation module was built around the central storage unit of the NWMO DGR design, namely the UFC and surrounding bentonite, 500 m below ground surface and, it is assumed, below the water table. Therefore, the pressure head is developed by the 500 m water column over the placement room. The model geometry is currently limited to two-dimensions (2D) due to the non-linear aspects of the Richards equation implementation. The 2D approximation of the placement room results in a loss of information, specifically at the hemi-spherical end caps and comparing results to the 3D modules should be done on a qualitative basis.

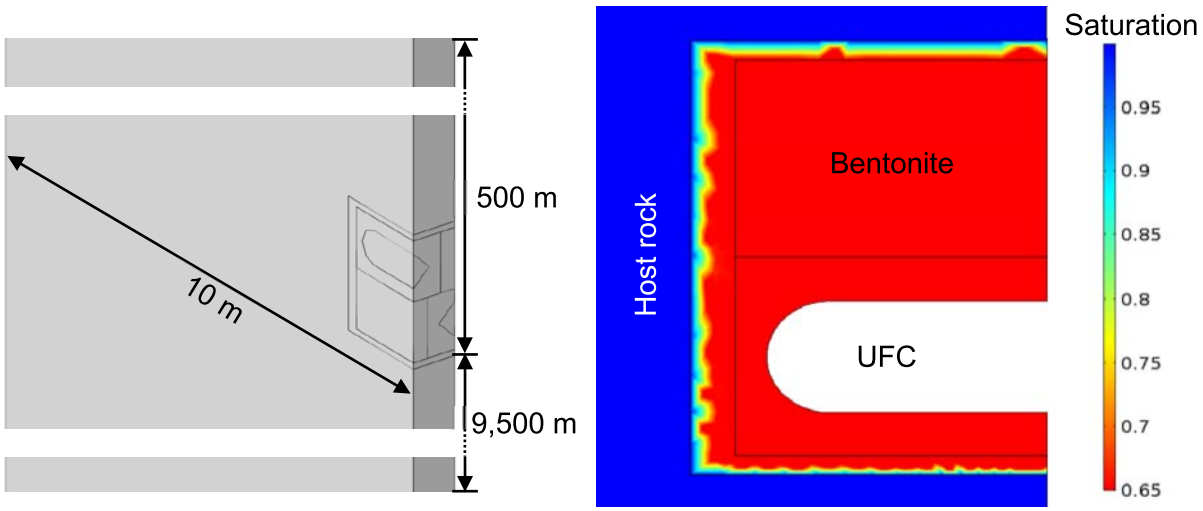



**Figure 11: A 2D model geometry on the right approximates the 3D DGR on the left. Saturation, representing initial conditions, is shown on the right image.**

The placement room profile (Figure 9) was used for the model, resulting in Figure 11. Figure 11 also shows the initial saturation conditions of the model, where the host rock is fully saturated and the bentonite is at 65% saturation. Similar to the diffusion module, the sulphide concentration is set to zero at the UFC surface and 1 ppm at the DGR-host rock interface. Similar to Module 2, the Richards equation module was meshed with finer elements closest to the UFC surface and larger elements moving away through the bentonite (Figure 12) and host rock.

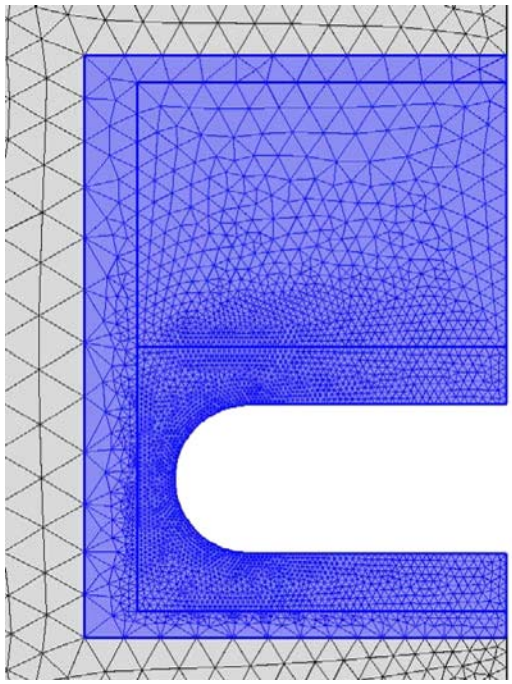


**Figure 12: Richards equation module mesh including 8443 elements with higher resolution in the placement room and a coarser mesh moving away from the DGR.**

## 5. RESULTS

The following section describes the results for the different modules. Similar to Section 4, the results for Section 5.1 have been published in Briggs et al., (2017b) and Briggs et al., (2017d), Section 5.2 in Briggs et al., (2017c) and Section 5.3 in Briggs et al., (2017a).

### 5.1 DIFFUSION MODULE RESULTS

#### 5.1.1 Validation Results

As an initial testing and validation stage, the diffusion model was compared with cases of known analytical solutions including 1D, 2D and 3D diffusion. For steady state 1D diffusion, Equation 5 becomes:

$$J = -D\frac{\Delta C}{\Delta x} \qquad \text{Equation 15}$$

where the flux [$NL^{-2}T^{-1}$] is defined across a concentration gradient $\Delta C$ [$NL^{-3}$] and a distance $\Delta x$ [L] for a known diffusion coefficient $D$ [$L^2T^{-1}$].

In 2D, a system with a known analytical solution was chosen, in this case, cylindrical shell diffusion, where a mass diffuses inwards from an outer shell to an inner shell boundary (Crank, 1975).

$$Q = \frac{2\pi hD(C_b - C_a)}{\ln(b/a)} \qquad \text{Equation 16}$$

where a mass, Q [$NT^{-1}$], diffuses through a shell with inner radius *a* [L] and outer radius *b* [L] with concentrations $C_a$ [$NL^{-3}$] and $C_b$ [$NL^{-3}$] respectively.

Finally, for 3D spherical shell diffusion was chosen for validation (Crank, 1975).

$$Q = 4\pi D \frac{ab}{b-a}(C_b - C_a) \qquad \text{Equation 17}$$

Validation against analytical solutions was successful and results are summarised in Table 4. An appropriate mesh size was assumed, as discussed in Section 4.1.

The 1D validation also included the original 1 mm reference MIC value which assumed a 40 cm bentonite cover including HCB and bentonite pellets (King, 1996). The reference corrosion value was also obtained through 1D COMSOL simulations using the assumed 1 ppm sulphide concentration used in this report and results in the expected value of 0.33 nm/year/ppm sulphide (Table 4) using Equation 4. The validation of the reference corrosion value indicates that similar assumptions have been made compared to previous studies with regard to effective diffusion coefficients, boundary conditions, system geometry, and physical processes.

**Table 4: Model Validation: Analytical vs. COMSOL**

| Model | Analytical Corrosion Rate (nm/year/ppm sulphide) | COMSOL Corrosion Rate (nm/year/ppm sulphide) |
|---|---|---|
| Reference MIC – 40 cm | 0.33 | 0.33 |
| 1D – Linear – 30 cm | 0.45 | 0.45 |
| 2D – Cylindrical Shell – 30 cm | 0.66 | 0.66 |
| 3D – Spherical Shell – 30 cm | 0.93 | 0.93 |

The diffusive flux through a 2D cylindrical shell was higher than the 1D linear diffusion (Table 4). This is due to the increased dimensionality of the problem and the change in geometry being modeled. As shown in Figure 13 the relative perimeter of the outer layer is larger than the inner perimeter and illustrates the complexities of radial diffusion concentrating towards cylindrical surfaces. Similarly, the 3D corrosion values were larger than the other results, again due to the change in dimensionality. The results indicate the importance of using 3D modelling for complex geometries, like those of the NWMO UFC.

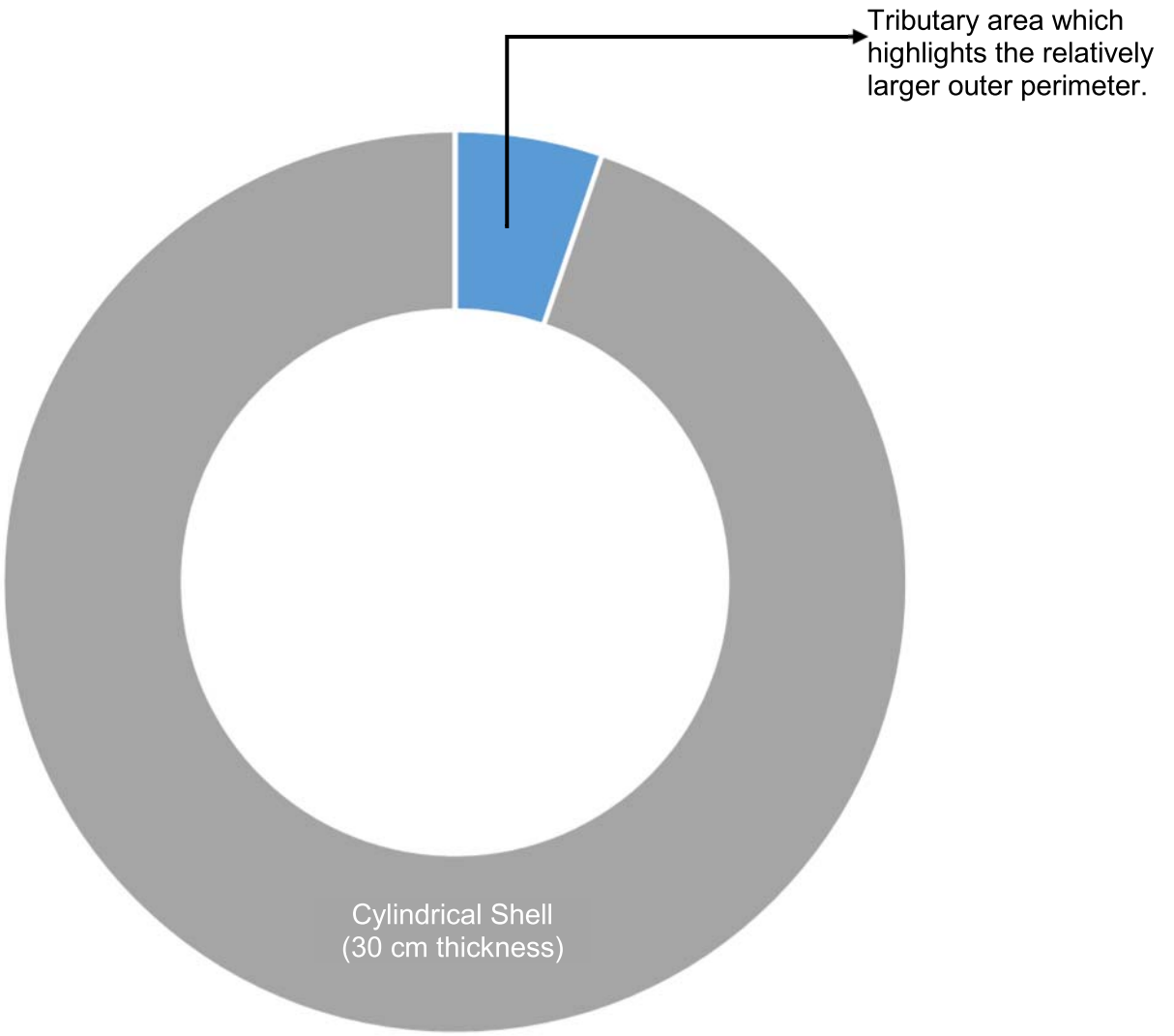



**Figure 13: Illustrative of 2D cylindrical shell diffusion with unit height, highlighting the larger outer perimeter of the bentonite cover. The figure illustrates the complexities of radial diffusion towards cylindrical surfaces.**

### 5.1.2 Modelling Results

Following validation of the developed system, the NWMO UFC package and placement room were modelled. For a simplified UFC package, including a single UFC and surrounding bentonite buffer with minimum 30 cm thickness, the average corrosion rate (across the whole surface) was calculated to be 0.65 nm/year/ppm sulphide. The maximum corrosion rate was 0.86 nm/year/ppm sulphide (Figure 14).

The corrosion rates calculated for multiple UFCs within a placement room were significantly reduced, compared to a single UFC package, to an average 0.31 nm/year/ppm sulphide across all UFCs (Table 5). This is due to the larger bentonite cover in the placement room. The largest corrosion rate was found at the hemi-spherical ends of each UFC and the worst-case corrosion rate was 0.76 nm/year/ppm sulphide (Figure 15), compared to 0.86 for a single UFC. The average corrosion rates are similar to the reference corrosion rate of 0.33 nm/year/ppm sulphide (Table 4) however, the average corrosion rates are not representative of the whole system as

sulphide flux varies across the modelled domain. The 3D model is required to capture the variation of sulphide flux across the system and to determine the maximum corrosion rates.

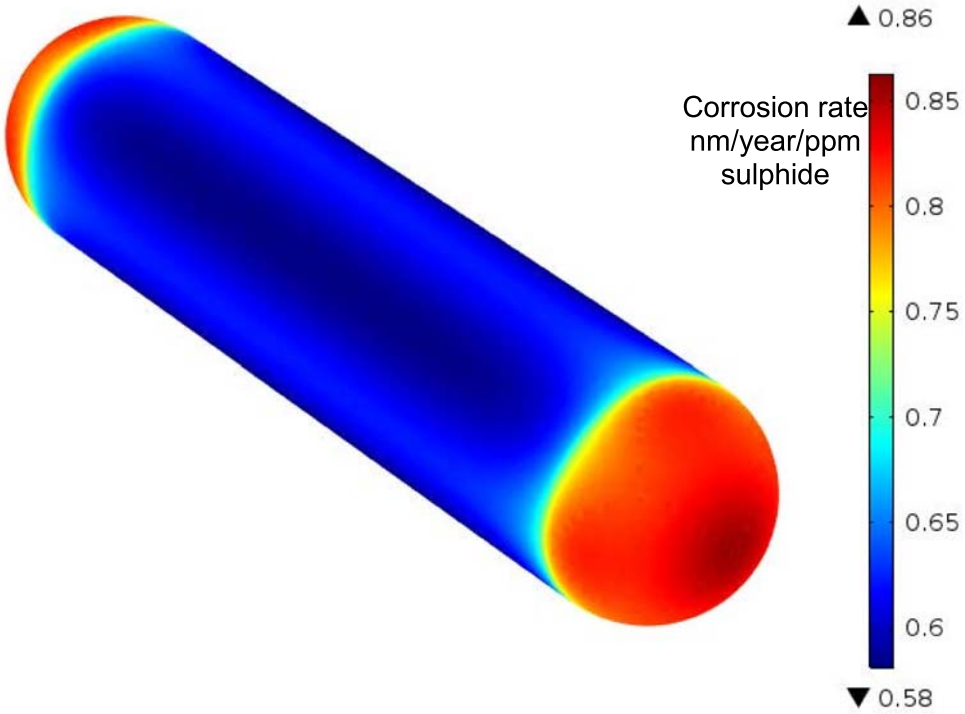



**Figure 14: Corrosion rate for the case of a single UFC package. Maximum corrosion occurs at the hemi-spherical end cap.**

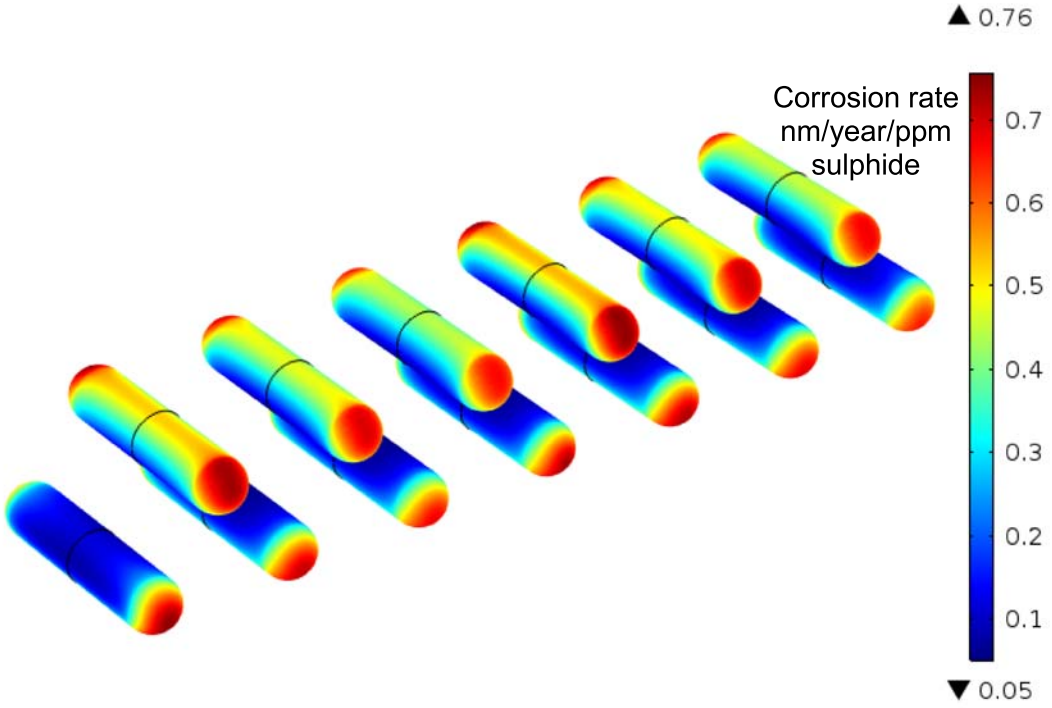



**Figure 15: Corrosion rate for the case of a 10 m segment of a placement room containing 13 UFCs.**

**Table 5: Corrosion rates for and UFC package and placement room**

| Model | Corrosion Rate (nm/year/ppm sulphide) |
|---|---|
| 3D – UFC package – minimum 30 cm bentonite | 0.65 (average), 0.86 (max.) |
| 3D – Placement room – minimum 30 cm bentonite | 0.31 (average), 0.76 (max.) |

The results given thus far represent the steady-state simulations, where sulphide is assumed to have already diffused through the bentonite buffer when the model is initialized. A more realistic scenario is that the concentration of sulphide in the EBS is initially zero, and over time sulphide diffuses through the EBS towards the UFC. Therefore, the steady state results are conservative. To improve on this conservative assumption, a time dependent solver was used to model the transient response of sulphide in the DGR over a 1 million year time span.

Results from the time dependent model show corrosion rates start from zero nanometers per year and increase over time until they reach the steady state condition. Both models reach steady state early, with the placement room reaching steady state sulphide concentrations after 2,000 years. This represents 0.2% of the total time span modelled and as such, it has little impact on the total corrosion depth of the UFC.

### 5.1.3 Sensitivity Analysis

A sensitivity analysis of the sulphide transport module was conducted by varying the diffusion coefficients and concentration gradients. For 3D geometries, when varying the diffusion coefficient and concentration gradients, the flux varies linearly as expected from analytical solutions (Equations 15 and 16). Figure 16 shows sensitivity of the effective sulphide diffusion coefficient from $10^{-12}$ to $10^{-9}$ $m^2/s$ and the resulting linear variation in the corrosion rate. Similarly, Figure 17 shows the linear variation in corrosion rate for changes in sulphide concentration gradients in the placement room geometry.

The final term of the diffusion equation relates to the geometry of the system. In 1D, it is the linear diffusion distance but in higher dimensions, it accounts for the shape (ie. cylindrical or spherical in the presented model) and is not always linearly related to the resulting flux. Therefore a 3D model is crucial in the design process as it will give the most accurate prediction of the repository,

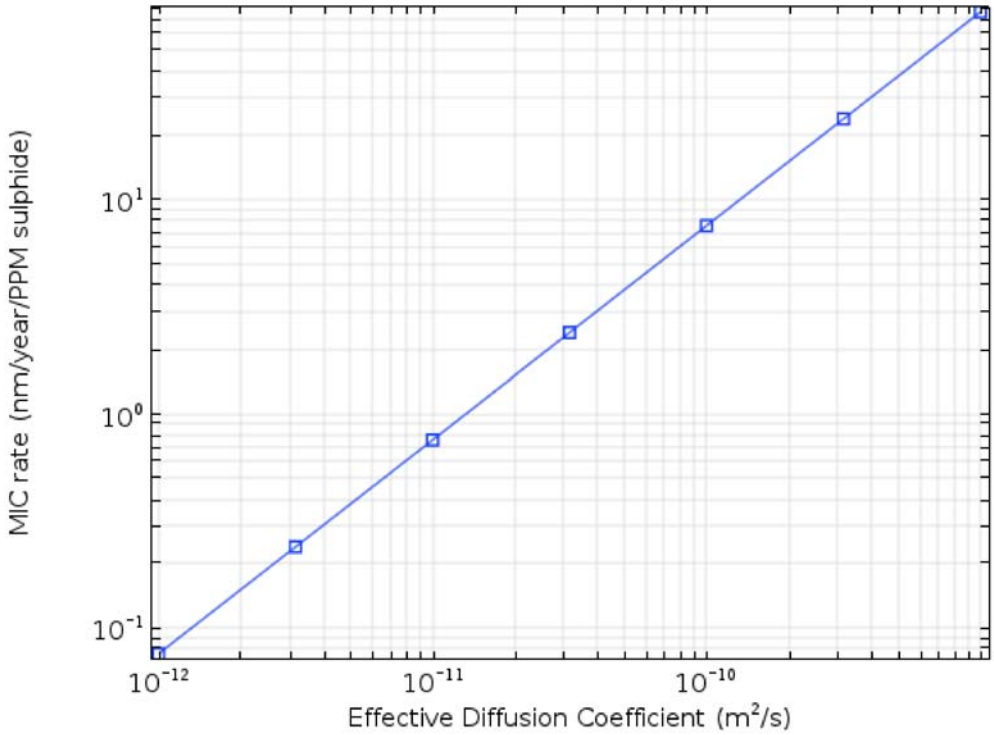



**Figure 16: Maximum corrosion rate for varying effective sulphide diffusion coefficients in the placement room geometry.**

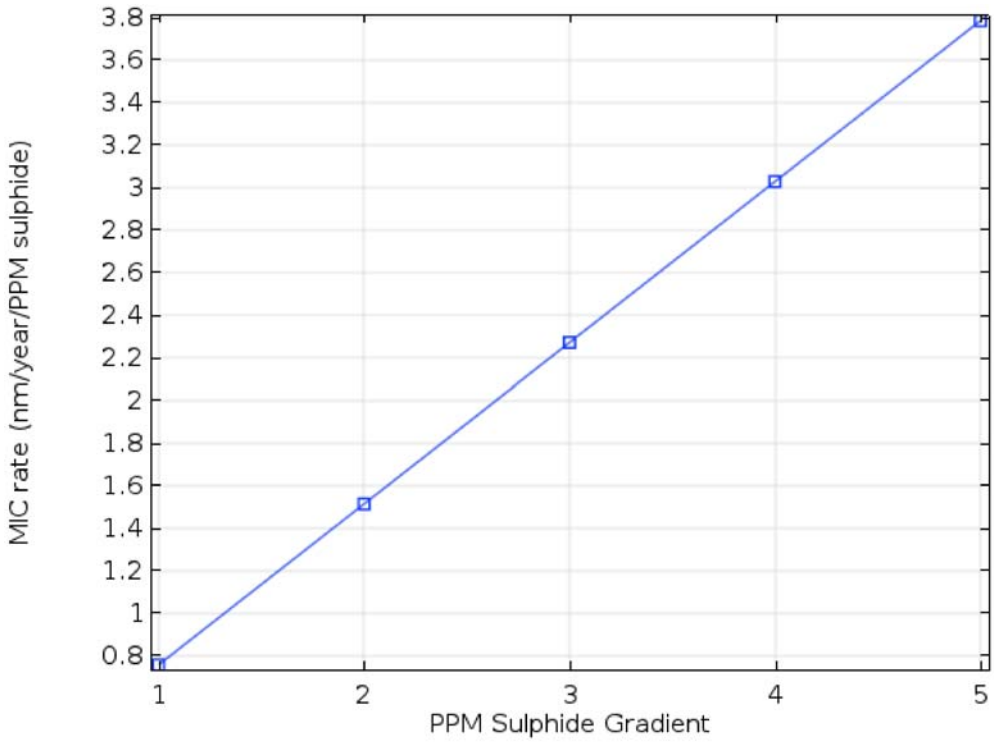



**Figure 17: Maximum corrosion rate for varying sulphide concentration gradients in the placement room geometry.**

## 5.2 THERMAL MODULE RESULTS

The thermal module was run for a reference period of 1 million years to determine the expected sulphide flux and corrosion rates at the UFC surface. Three versions of the thermal DGR model were simulated. The first scenario modelled the geosphere at a constant temperature of 25°C, the temperature assumed for previous models in this report. The second scenario was modelled at the expected long-term repository temperature of 11°C and finally the third scenario simulated a temperature dependent scenario, where temperature fluctuated due to the heating of the UFC.

The geometry in the thermal module differs from that of the diffusion module as described in Section 4.1 and 4.2. The diffusion module captures a larger segment of a placement room, including 13 UFC packages. However, since the thermal module includes several hundred meters of surrounding host rock, it becomes necessary to narrow the placement room being modelled to only a quarter of two UFC packages. Therefore, even though the diffusion model already simulated a scenario at 25°C in the previous section, it was completed for a different geometry and therefore the thermal module was also simulated at a constant 25°C, as a measure of validation. It was found that the maximum corrosion rate at 25°C was 0.77 nm/year/ppm of sulphide which is within 1% of the corrosion rate for the diffusion module (Table 5).

The maximum value drops to 0.52 nm/year/ppm of sulphide when the temperature is assumed to be 11°C (Figure 18) representing a reduction over the 25°C case. The isothermal model of the DGR simulates the ingress of sulphide reaching steady state concentrations in approximately 2,000 years (Figure 19).

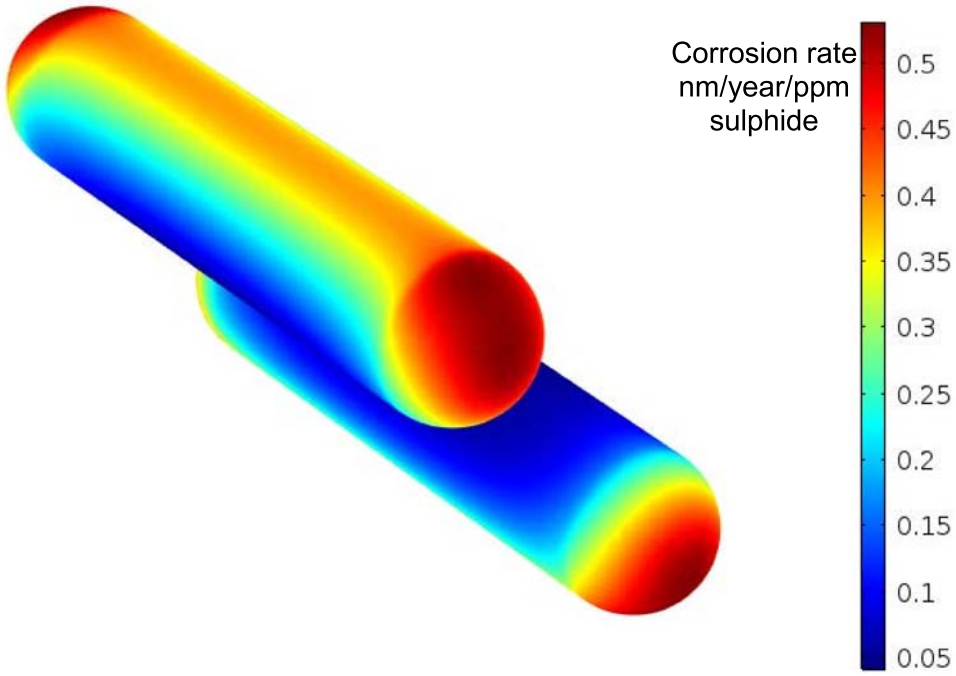



**Figure 18: Corrosion rate calculated from sulphide flux at the UFC surface for isothermal conditions at 11°C.**

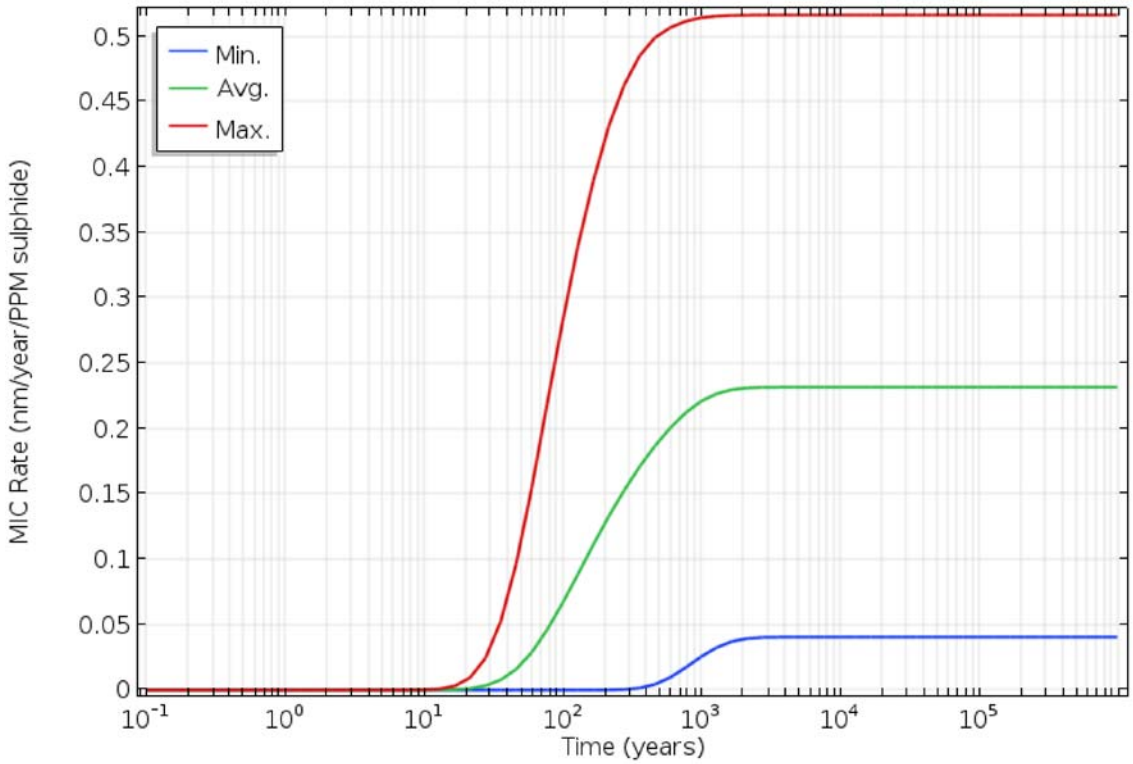



**Figure 19: Time dependent corrosion rate calculated from sulphide flux for the isothermal model at 11°C over 1,000,000 years. Minimum flux occurs at the inner UFC surface (between two containers) while the maximum flux occurs at the hemi-spherical end caps.**

The thermal DGR model includes the host rock and the heat output of the used nuclear fuel. Results from this model show a varying temperature profile over time (Figure 20) reaching a maximum temperature of 85°C at approximately 30 years after placement. The second temperature peak in Figure 18 is a result of the boundary conditions used in the model and is not representative of the physical system (Guo, 2017). The use of two symmetry planes, one on each side of the placement room effectively represents an infinite number of UFC heat sources. Therefore, the heat from the UFCs reflects on itself an infinite number of times resulting in a secondary heating of the DGR at approximately 1,000 years.

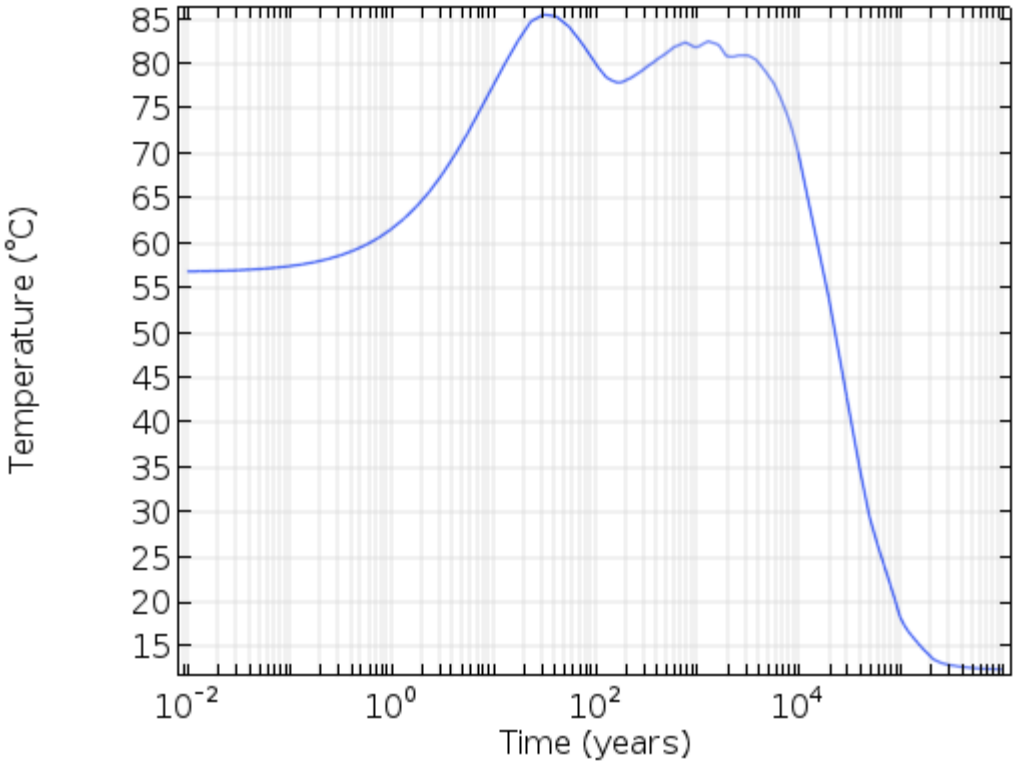



**Figure 20: Temperature dependent model showing the average UFC surface temperature over 1,000,000 years.**

Guo (2017) has shown the physical system to have one peak that is accurately predicted by the existing model and followed by a continuous drop in temperature over time. The thermal module used in this report over-predicts the temperatures between years 200 and 20,000 and consequently over-predicts sulphide flux during this time. Therefore, for the purposes of determining sulphide transport with respect to the corrosion rate, this is a conservative result.

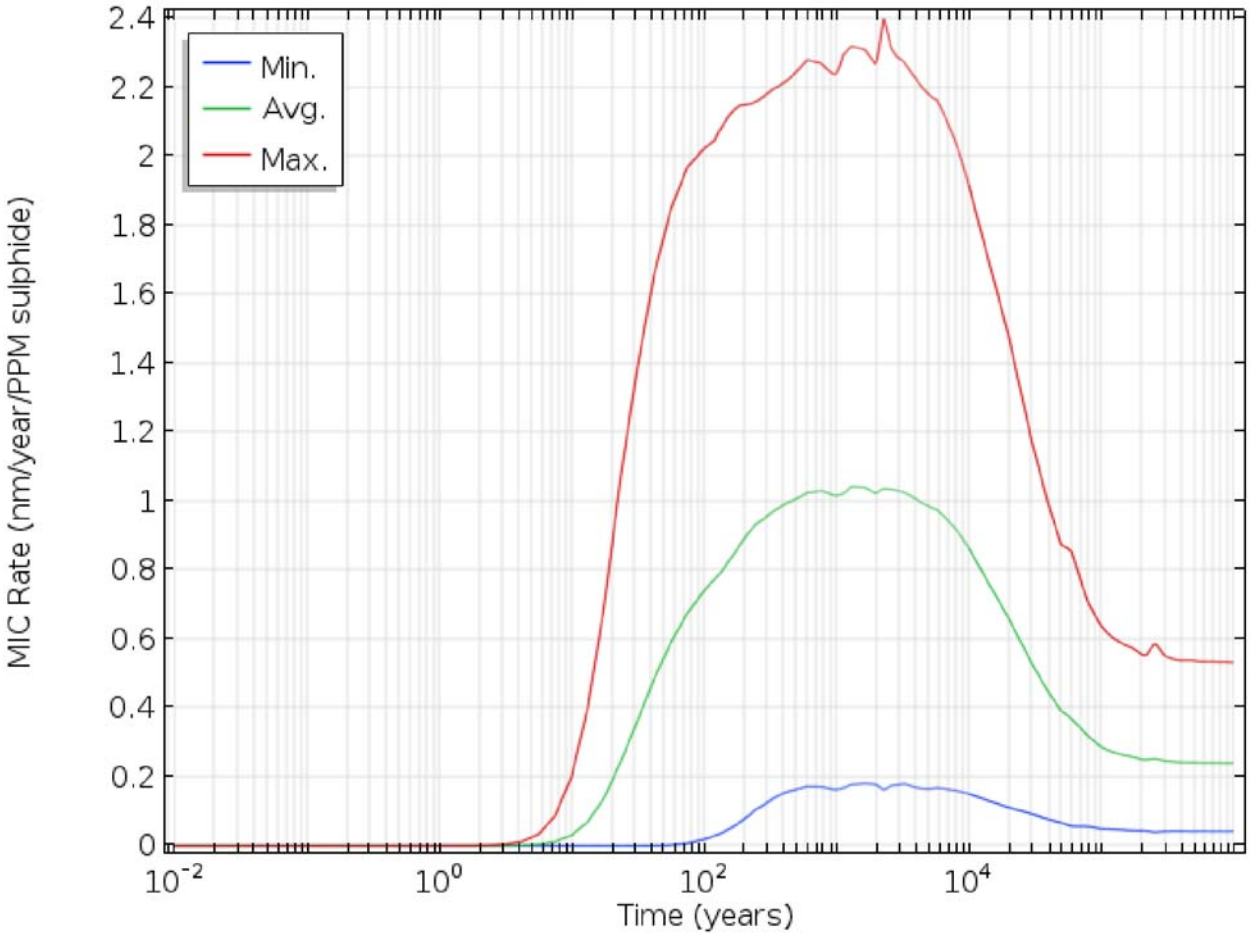



**Figure 21: Time and temperature dependent corrosion rates in the DGR for the thermal module. For the maximum reported values (red line), corrosion rates peak around 1,000 years at 2.48 nm/year/ppm sulphide then drop to a steady state value of 0.53.**

Figure 21 reports the corrosion rate for the thermal module over a 1 million year span. Similar to Figure 17, minimum, average and maximum UFC surface values are reported. The steady state corrosion rate (at 1 million years) of the UFC was calculated and compared in Table 6.

**Table 6: Corrosion rates for thermal module**

| Condition | Steady State Corrosion Rate at 1 million years (nm/year/ppm sulphide) |
|---|---|
| Isothermal, 25°C | 0.32 (average), 0.77 (max.) |
| Isothermal, 11°C | 0.23 (average), 0.52 (max.) |
| Thermal | 0.24 (average), 0.53 (max.) |

As seen from Table 6, the time dependent thermal model calculates a corrosion rate of 0.53 nm/year/ppm sulphide at 1 million years. This shows that there is a marginal increase of total sulphide arriving at the UFC surface when the additional effects of temperature are considered in the NWMO DGR, compared to the isothermal base case at 11°C. In addition, the maximum rate

peaks at an earlier time (around 1,000 years) with a value of 2.48 nm/year/ppm sulphide. The integrated thermal model maximum corrosion rate over the 1 million year span of the model results in 0.60 mm total depth of corrosion compared to 0.52 mm for the isothermal base case at 11°C. Temperature effects are discernable over the time scales of the simulation but still less than the conservative case modelled in Section 5.1 that resulted in 0.76 mm over a 1 million year time period.

## 5.3 RICHARDS EQUATION MODULE RESULTS

The Richards Equation module assumes an initial bentonite saturation of 65% and the outer perimeter (host rock) at 100% saturation. The model simulated water movement from the wet host-rock towards the UFC surface. All simulations were performed under isothermal (25°C) conditions.

Initially, copper corrosion rates at the UFC surface were zero since no sulphide was present at the container. As the placement room became water saturated, pathways developed between the host-rock and UFC surface allowing for diffusion of sulphide to the container. The first water saturated pathway occurred at the hemi-spherical end caps around 200 years, while full saturation of the placement room did not occur until 2,000 years.

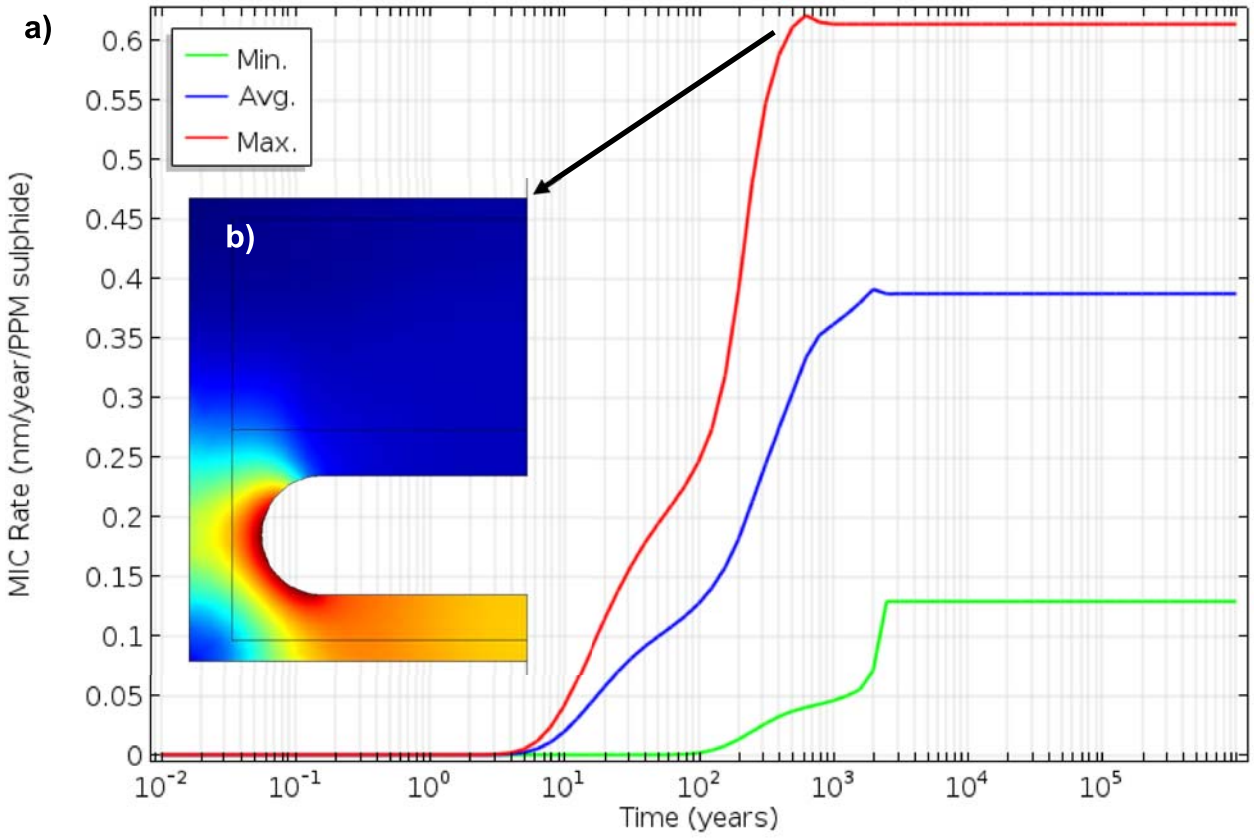



**Figure 22: a) Corrosion rate for 1 ppm sulphide concentration gradient for a hydraulic conductivity of $10^{-14}$ m/s b) Sulphide flux profile through placement room at peak corrosion rate (red indicates higher flux while blue indicates lower flux).**

Figure 22 shows the maximum corrosion rate at the UFC surface as a function of sulphide flux for a hydraulic conductivity of $10^{-14}$ m/s. The maximum sulphide flux occurred at the hemi-spherical end caps, similar to earlier results presented in this report. The peak flux occurred at

600 years resulting in a maximum corrosion rate of 0.62 nm/year/ppm of sulphide. This condition lasted a few years until a steady state corrosion rate of 0.61 nm/year/ppm sulphide was maintained. However, the diffusion module resulted in a maximum steady state corrosion rate of 0.76 nm/year/ppm sulphide as reported earlier, the discrepancy is likely related to the 2D implementation of the Richards equation module, where lower flux values are expected (as discussed in Section 5.1).

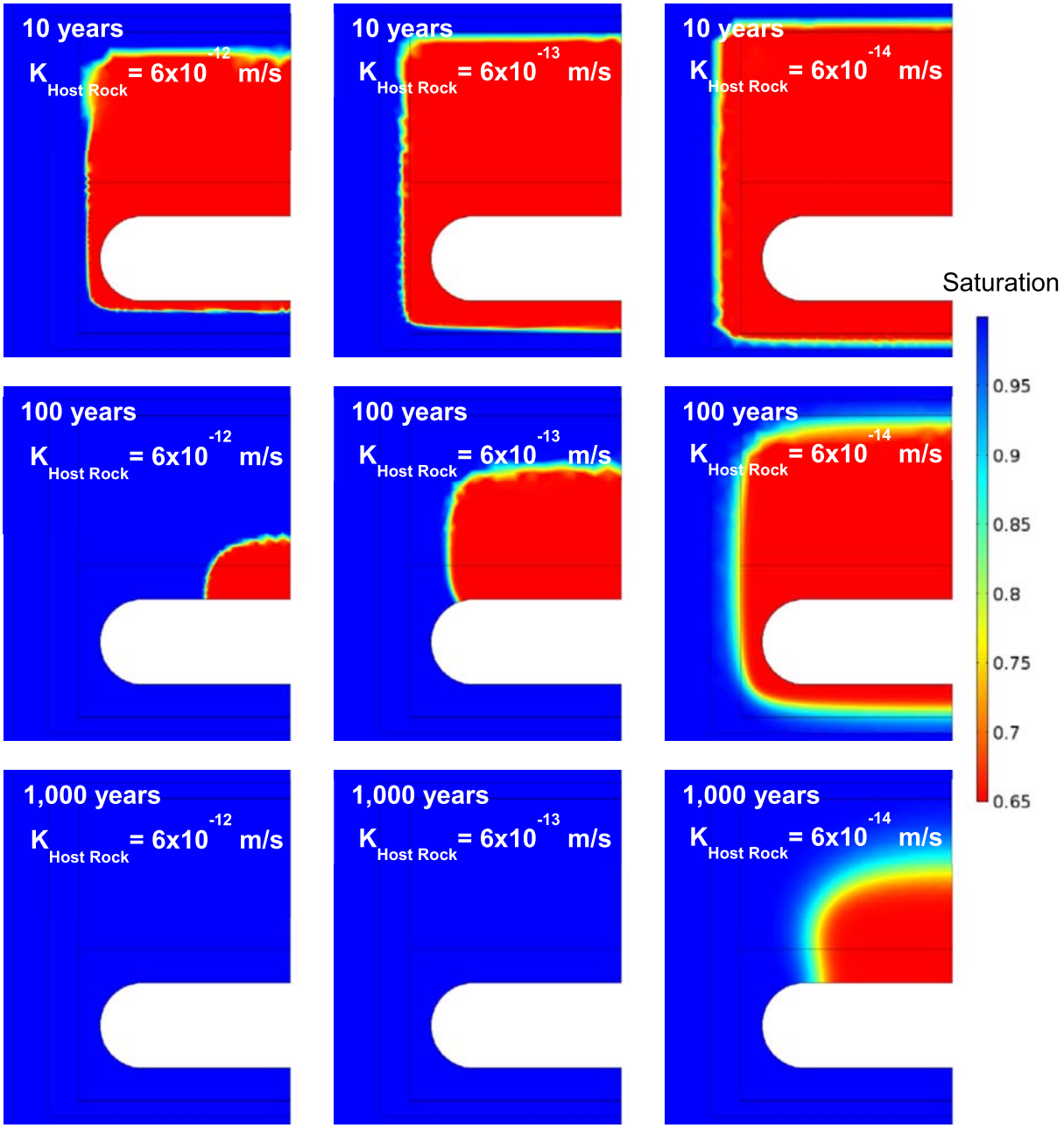



**Figure 23: Saturation at 10, 100 and 1,000 years for varying hydraulic conductivities.**

Sensitivity analysis of the host rock hydraulic conductivity showed a significant effect on the rate of saturation. Figure 23 shows the sensitivity analysis over two orders of magnitude for the host rock hydraulic conductivities. The largest value, on the order of $10^{-12}$ m/s, represents a crystalline

host rock with moderate connectivity of discrete fractures. While the lowest value, $10^{-14}$ m/s, indicates a largely intact crystalline host rock (Sykes et al., 2011).

## 6. DISCUSSION AND FUTURE WORK

This report describes development of a 3D numerical model using COMSOL to estimate MIC of the UFC in a DGR environment. Sulphide transport was modelled under three conditions, or modules: isothermal and fully saturated, non-isothermal and fully saturated, and isothermal and variably saturated. The diffusion of corrosive species through the EBS was simulated in all three cases and the results matched well to analytical solutions developed under isothermal and saturated conditions. 3D modelling of the EBS showed that the maximum corrosion rate, due to MIC, on the UFC surface may be up to 0.76 nm/year/ppm sulphide at steady state. These results are for an assumed concentration boundary condition of 1 ppm and therefore do not represent the site-specific conditions. The developed model will be refined as design-specific information becomes available and will incorporate site-specific data through the NWMO site selection process.

The results presented in this report indicate that extent of corrosion from sulphide diffusion may not be uniform over the container, as assumed by initial scoping calculations. The hemi-spherical UFC end caps were predicted to have the highest values of corrosion, over 2.4 times that of the average corrosion rates. This results from the unique geometry of the placement room and UFC resulting in complex sulphide diffusion pathways moving radially inwards to concentrate on the hemi-spherical UFC end caps. This phenomenon could not have been observed previously using 1D calculations and therefore future work investigating sulphide diffusion through NWMO EBS should continue to incorporate 3D modelling.

The thermal module captured the time dependent nature of the sulphide flux, as a result of the changing thermal load due to the used nuclear fuel. Heat from the spent fuel warms the DGR during the first 100 years then it cools over the following 200,000 years to background temperatures. Maximum corrosion rates, at the hemi-spherical end caps, reached steady-state at 0.53 nm/year/ppm sulphide. While the integrated maximum corrosion rate was 0.60 mm over the 1 million year time span of the model. Temperature effects are discernable over the time scales of the simulation but still less than the conservative case modelled in Section 5.1 that resulted in 0.76 mm/year/ppm sulphide.

The Richards equation module implemented in 2D included a cross-section of a UFC package and the surrounding bentonite and host rock. It was used to model the movement of water into the DGR. While the results of the 2D Richards equation module are not directly comparable to the 3D results reported earlier there are still insights to be gained. Results indicate a large variability in saturation time which is sensitive to the hydraulic conductivity of the host rock. The model predicts full saturation of the DGR at approximately 2,000 years with the first saturated pathways to the UFC surface around 200 years. As reported, 3D modelling is required to capture the effects of sulphide flux at the hemi-spherical end caps and as the 3D Richards module is implemented more direct comparison will be possible.

In summary, it was found that COMSOL, a physics modelling package, is well suited for simulating steady state and time dependent diffusive transport in complex geometries under isothermal, thermal, and variably-saturated conditions. Future work includes the addition of geochemical reactions to the model, 3D implementation of variably saturated module, coupled thermal effects with variably saturated module, incorporation of corrosion equations, potential microbial reactions, and biochemical modelling.

**ACKNOWLEDGMENTS**

Research reported in this publication was supported by MITACS and NWMO who provide project funding through York University. The authors would like to acknowledge Brent Sleep (University of Toronto) for his insight and contributions during the development of the Diffusion Module. The thoughtful peer-review by Dr. Joe Small and Dr. Liam Abrahamsen-Mills of the Nuclear National Laboratories, United Kingdom, is gratefully acknowledged.

## REFERENCES

Alt-Epping, P., Tournassat, C., Rasouli, C., Steefel, C.I., Mayer, K.U., Jenni, A., Mader, U., Sengor, S.S. & Fernandez, R (2015). Benchmark reactive transport simulations of a column experiment in compacted bentonite with multispecies diffusion and explicit treatment of electrostatic effects. Computational Geoscience, 19, 535-550.

Appelo, C.A.J. (2013). A review of porosity and diffusion in bentonite. Working Report 2013-29. POSIVA, Olkiluoto.

Appelo, C.A.J., Van Loon, L. R., & Wersin, P. (2010). Multicomponent diffusion of a suite of tracers (HTO, Cl, Br, I, Na, Sr, Cs) in a single sample of Opalinus Clay. Geochimica et Cosmochimica Acta, 74(4), 1201-1219.

Baumgartner, P., Tran, T.V., & Burgher, R. (1994). Sensitivity Analyses for the Thermal Response of a Nuclear Fuel Waste Disposal Vault. TR-621-COG-94-258. Atomic Energy of Canada Limited. Pinawa, Manitoba

Baumgartner, P., (2006). Generic thermal-hydraulic-mechanical (THM) data for sealing materials, Volume 1: soil-water relationship. 06819-REP-01300-10122-R00. Ontario Power Generation, Nuclear Waste Management Division. Toronto, Ontario

Bear, J., (2012). Hydraulics of groundwater. Courier Corporation.

Bengtsson, A., & Pedersen, K. (2017). Microbial sulphide-producing activity in water saturated Wyoming MX-80, Asha and Calcigel bentonites at wet densities from 1500 to 2000kgm−3. Applied Clay Science, 137, 203-212.

Bojinov, M., & Mäkelä, K. (2003). Corrosion of copper in anoxic 1M NaCl solution. Working Report 2003-45. Posiva, Olkiluoto.

Bourg, I.C., Sposito, G., & Bourg, A.C.M. (2008). Modeling the diffusion of Na+ in compacted water-saturated Na-bentonite as a function of pore water ionic strength. Applied Geochemistry, 23, 3635-3641.

Bradbury, M.H. & Baeyens, B. (2003). Porewater chemistry in compacted re-saturated MX-80 bentonite. Journal of Contaminant Hydrology, 61, 329-338.

Briggs, S., Birch, K., & Krol, M. (2017a). Transport modelling of corrosive agents through a variably saturated bentonite buffer. In Proceeding of The Canadian Geotechnical Society – GeoOttawa 2017 Conference, October 1 – 4, 2017, Ottawa, Ontario.

Briggs, S., McKelvie, J., Keech, P., Sleep, B., & Krol, M. (2017b). Transient modelling of sulphide diffusion under conditions typical of a deep geological repository. Corrosion Engineering, Science and Technology, 1-4.

Briggs, S., McKelvie, J., & Krol, M. (2017c). Temperature dependent sulphide transport in highly compacted bentonite. In Proceedings of the International High-Level Radioactive Waste Management (IHLRWM 2017) Conference, April 9 – 13, 2017, Charlotte, NC

Briggs, S., McKelvie, J., Sleep, B., & Krol, M. (2017d). Multi-dimensional transport modelling of corrosive agents through a bentonite buffer in a Canadian deep geological repository. Science of The Total Environment, 599, 348-354.

Chen, J., Qin, Z., & Shoesmith, D. W. (2011). Long-term corrosion of copper in a dilute anaerobic sulfide solution. Electrochimica Acta, 56(23), 7854-7861.

Crank, J. 1975. The Mathematics of Diffusion. Clarendon Press, Oxford, Brunel University, Uxbridge.

Einstein, A. (1905), Über die von der molekularkinetischen Theorie der Wärme geforderte Bewegung von in ruhenden Flüssigkeiten suspendierten Teilchen. Ann. Phys., 322: 549–560. doi:10.1002/andp.19053220806

Gascoyne, M. (1997). Evolution of Redox Conditions and Groundwater Composition in Recharge-Discharge Environments on the Canadian Shield. Hydrogeology Journal. 5. 4-18.

Glaus, M.A., Frick, S., Rosse, R., & Van Loon, L.R. (2011). Consistent interpretation of the results of through-, out-diffusion and tracer profile analysis for trace anion diffusion in compacted montmorillonite. Journal of Contaminant Hydrology, 123, 1-10.

Guo, R. (2017). Thermal response of a Canadian conceptual deep geological repository in crystalline rock and a method to correct the influence of the near-field adiabatic boundary condition. Engineering Geology, 218, 50-62.

Hall, D, Standish, T., Keech, P., and Boyle, C. (2017). The oxic copper corrosion allowance of the conceptual NWMO Mark II crystalline deep geological repository. APM-CALC-03220-0203. Nuclear Waste Management Organization. Toronto, Ontario, Canada.

Huber, M.L., Perkins, R.A., Laesecke, A., Friend, D.G., Sengers, J.V., Assael, M.J., ... & Miyagawa, K. (2009). New international formulation for the viscosity of H2O. Journal of Physical and Chemical Reference Data, 38(2), 101-125.

Idemitsu, K., Kozaki, H., Yuhara, M., Arima, T., & Inagaki, Y. (2016). Diffusion behavior of selenite in purified bentonite. Progress in Nuclear Energy, 92, 279-285.

Ikeda, B.M, and Litke, C.D. (2007). Stress Corrosion Cracking of Copper in Nitrite/Chloride Mixtures at Elevated Temperatures. TR-2007-04. Nuclear Waste Management Organization. Toronto, Ontario

Ikeda, B.M, and Litke, C.D. (2008). The Effect of High Chloride Concentration on Stress Corrosion Cracking Behaviour of Copper. TR-2008-12. Nuclear Waste Management Organization. Ontario, Canada

Johansson, A.J., Lilja, C., and Brinck, T. (2012). On the Formation of Hydrogen Gas on Copper in Anoxic Water. Journal of Chemical Physics. 135, 084709.

King, F., (1996). Microbially Influenced Corrosion of Copper Nuclear Fuel Waste Containers in a Canadian Disposal Vault. AECL-11471. Atomic Energy of Canada Ltd. Pinewa, Manitoba

[1]King, F. and M. [2]Kolar. (2006). Consequences of microbial activity for corrosion of copper used fuel containers –analyses using the CCM-MIC.0.1 code. Prepared by [1]Integrity Corrosion Consulting, Ltd and [2]LS Computing Ltd. 06819-REP-01300-10120-R00. Ontario Power Generation, Nuclear Waste Management Division. Toronto, Ontario

Kremer, E.P. (2017). Durability of the Canadian used fuel container. Corrosion Engineering, Science and Technology, 52(sup1), 173-177.

Kwong, G. (2011). Status of Corrosion Studies for Copper Used Fuel Containers Under Low Salinity Conditions. TR-2011-14.Nuclear Waste Management Organization. Toronto, Ontario.

Lide, D.R., & Haynes, W.M. (2009). CRC handbook of chemistry and physics: a ready-reference book of chemical and physical data-/editor-in-chief, David R. Lide; ass. ed. WM Mickey Haunes. Boca Raton, Fla: CRC.

Litke, C.D and Ikeda, B.M. (2008). The Stress Corrosion Cracking Behaviour of Copper in Acetate Solutions. TR-2008-21. Nuclear Waste Management Organization. Toronto, Ontario

Litke, C.D. and Ikeda, B.M. (2011). Status Report on Stress Corrosion Cracking Behaviour of OFP Copper in Nitrite and Ammonia Solutions. TR-2011-06. Nuclear Waste Management Organization. Toronto, Ontario

Martin, M., Cuevas, J., & Leguey, S. (2000). Diffusion of soluble salts under a temperature gradient after the hydration of compacted bentonite. Applied clay science, 17(1), 55-70.

Millington, R. J., & Quirk, J. P. (1961). Permeability of porous solids. Transactions of the Faraday Society, 57, 1200-1207.

NWMO, (2013). Mark II Design Concept for Crystalline and Sedimentary Host Rock. APM-PDD-04000-0003. Nuclear Waste Management Organization. Toronto, Ontario.

Oscarson, D. W., Hume, H. B., & King, F. (1994). Sorption of cesium on compacted bentonite. Clays and Clay Minerals, 42(6), 731-736.

Ottosson, M., Boman, M., Berastegui, P., Andersson, Y., Hahlin, M., Korvela, M. (2017). Copper in Ultrapure Water, a Scientific Issue Under Debate. Corrosion Science 122, 53-60.

Scully, J. and Edwards, M. (2013). Review of the NWMO Copper Corrosion Allowance. TR-2013-04. Nuclear Waste Management Organization. Toronto, Ontario.

SKB, (2010). Corrosion calculations report for the safety assessment SR-Site. SKB-TR-10-66. Swedish Nuclear Fuel and Waste management Co. Stockholm, Sweden.

Stroes-Gascoyne, S., Hamon, C., Maak, P., and Russell, S. (2010). The effects of the physical properties of highly compacted smectitic clay (bentonite) on the culturability of indigenous microorganisms. Applied Clay Science, 47(1), 155-162.

Sykes, J. F., Normani, S. D., & Yin, Y. (2011). Hydrogeologic modelling. DGR-TR-2011-16, Nuclear Waste Management Organization, Toronto, Canada.

Tait, J.C., Roman, H., Morrison, C.A., (2000). Characteristic and radionuclide inventories of used fuel from OPG Nuclear Generation Stations. Volume 1 – Main report; and Volume 2 – Radionuclide inventory data. 06819-REP-01200-10029-R00. Ontario Power Generation, Nuclear Waste Management Division. Toronto, Canada.

van Genuchten, M.T., (1980). A closed-form equation for predicting the hydraulic conductivity of unsaturated soils. Soil science society of America journal, 44(5), pp.892-898.

Van Loon, L.R, Glaus, M.A., & Muller, W. (2007). Anion exclusion effects in compacted bentonites: Towards a better understanding of anion diffusion. Applied Geochemistry, 22, 2536-2552.

Wersin, P., Alt-Epping, P., Pekala, M., Pitkänen, P., & Snellman, M. (2017). Modelling Sulfide Fluxes and Cu Canister Corrosion Rates in the Engineered Barrier System of a Spent Fuel Repository. Procedia Earth and Planetary Science, 17, 722-725.